

UNIVERSITY OF TWENTE

BACHELOR ASSIGNMENT

Temperature optimization of the
SuperParamagnetic Quantifier for
comparison with standard methods

Jeroen Schlief (s1589504)
Advanced Technology

June 22, 2017

Bachelor assignment committee:
Chairperson: Dr. ir. B. ten Haken
Supervisor: M.M. van de Loosdrecht, MSc
External member: Dr. H.K. Hemmes

Abstract

For use in sentinel lymph node biopsies, a hand held probe has been developed to detect superparamagnetic nanoparticles using Differential magnetometry. The SuperParamagnetic Quantifier (SPaQ) is designed to find suitable particles to be used with the hand held probe. Additionally, it can quantify the amount of nanoparticles in a sample. The system's temperature dependency is determined to compare it to Vibrating Sample Magnetometry (VSM) and Magnetic Particle Spectroscopy (MPS). Measurements with the system in thermal equilibrium return a constant dM/dH curve where some drift occurs. For this drift is corrected using a fit of the Langevin function. The VSM determines the static magnetization curve, as little relaxation occurs. MPS results in the dynamic dM/dH curve, dependent on the used field amplitude and frequency. SPaQ's output curves could be considered a hybrid of a dynamic and a static dM/dH curve. Thus resulting in the conclusion that SPaQ is most suitable for its intended purpose.

Contents

1	Introduction	3
2	Background	4
2.1	Sentinel lymph node biopsy	4
2.1.1	Handheld probe	5
2.2	SuperParamagnetic Quantifier (SPaQ)	5
2.2.1	SuperParamagnetic Iron Oxide Nanoparticles (SPIONs)	6
2.2.2	Differential magnetometry	8
2.2.3	dM/dH curve determination	9
2.2.4	dM/dH curve analysis	10
3	Temperature optimization of SPaQ	12
3.1	Temperature dependency	12
3.2	Determination of temperature dependency	14
3.2.1	Methods	14
3.2.2	Results and discussion	15
3.3	Data compensation for fit	17
4	SPaQ compared to Vibrating Sample Magnetometry	21
4.1	Vibrating Sample Magnetometer	21
4.2	Sample preparation	21
4.3	Methods	22
4.4	Results and discussion	22
5	SPaQ compared to Magnetic Particle Spectroscopy	27
5.1	Magnetic Particle Susceptibility	27
5.2	Methods	28
5.3	Results and discussion	28
6	AC Susceptibility and Magnetorelaxometry for SPION analysis	32

7 Discussion	33
8 Conclusion	35
9 Recommendations	36
9.1 Further comparison	36
9.2 Measurement sequence	36
9.3 SuperParamagnetic Quantifier	37
10 Acknowledgements	39
References	39
List of Figures	41
List of Tables	42
A Temperature measurements	43

1 Introduction

The sentinel lymph node biopsy is a medical procedure used to determine the stage of certain cancers. This procedure requires the use of a radioactive tracer and a gamma probe to detect the tracer. Recently the Magnetic Detection & Imaging (MD&I) group at the University of Twente developed a hand held probe to replace aforementioned gamma probe. As this probe relies on the magnetic behaviour of the tracer to be able to detect it, the radioactive tracer is replaced by Superparamagnetic Iron Oxide Nanoparticles (SPIONs) [1].

Opposed to a previously developed hand held probe, the sentimag, the new hand held probe employs Differential Magnetometry (DiffMag) [2]. This technique relies on the nonlinear magnetization curve of superparamagnetic materials to distinguish the particles from the diamagnetic tissue.

Closely related to this hand held probe, is the SuperParamagnetic Quantifier (SPaQ). This system's purpose, is to find a suitable nanoparticle to be used in the sentinel lymph node biopsy. For this purpose, the dM/dH curve of a sample can be determined for low fields.

Additionally, the SPaQ is able to quantify the amount of SPIONs in a sample. While the height of the dM/dH curve is indicative of this, the SPaQ is also able to employ the DiffMag protocol as used in the hand held probe. However, one should not confuse the determination of the dM/dH curve with Differential Magnetometry as these are different procedures [3].

Similar to SPaQ are the Vibrating Sample Magnetometer (VSM) and Magnetic Particle Spectrometer (MPS). These systems are able to measure the magnetization curve and dM/dH curve respectively. The goal of this report is, to compare SPaQ to both VSM and MPS regarding the purpose of SPaQ as mentioned before [4][5][6].

However, before these systems can be compared, SPaQ should produce reproducible results. As of now, this is not the case. Although measurements of the same sample result in similar dM/dH curves, these are not identical. Most noticeable is the vertical drift of the dM/dH curves. It is hypothesized, that these observations are caused by temperature effects. Section 3 will treat the determination of this temperature dependency, as well as the optimization of SPaQ. This optimization is further discussed in the recommendations.

For the comparison of SPaQ with MPS, the Magnetic Particle Spectrometer of the Institut für Elektrische Messtechnik und Grundlagen der Elektrotechnik group at the Technical University of Braunschweig was used. This group also makes use of AC Susceptibility (ACS) and Magnetorelaxometry (MRX) to analyse SPIONs. This report will only briefly touch upon these systems, as its main focus is the comparison with VSM and MPS.

The comparison of SPaQ to VSM and MPS is both practical and theoretical. Measurement results of all systems are discussed. Furthermore, the differences in physical principles of all systems are emphasized. Here, the static magnetization curve and dynamic magnetization curve should be distinguished.

Based on the Magnetic Particle Spectrometer, recommendations are made regarding both the sequence used in SPaQ to determine dM/dH , as well as several hardware improvements.

2 Background

2.1 Sentinel lymph node biopsy

At the foundation of the SuperParamagnetic Quantifier lies a clinical case. This is the medical procedure known as the sentinel lymph node biopsy (SLNB) [1]. This procedure is used to determine the stage of certain cancers such as breast cancer [7].

Lymph nodes are part of the lymphatic system which transports lymph through the body as part of the immune system. As tumor cells break off a (breast) tumor and metastasize, the sentinel lymph node is the first lymph node most likely for the metastases to end up, as many cancerous cells spread through the lymphatic system. Therefore, the knowledge whether cancerous cells are present in the sentinel lymph node, offers insight in the stage the cancer is in. As the name suggests, a sentinel lymph node biopsy is a procedure in which this node is identified and excised. As can be seen in figure 1.

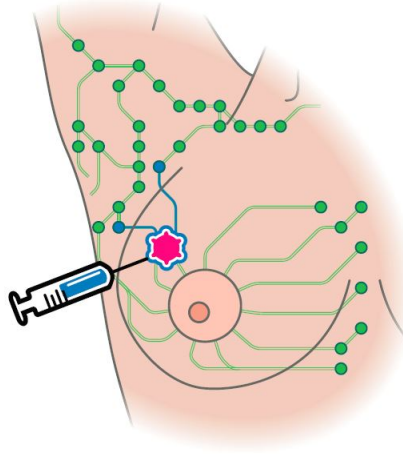


Figure 1: Principle of a sentinel lymph node biopsy. A dye and tracer are injected at the tumor location and travel through the lymphatic system towards the sentinel lymph nodes, indicated in blue [1].

Near the primary tumor, a blue dye and/or a radioactive tracer are injected. Usually Technetium ^{99m}Tc macro aggregated albumin is used. As potential metastases would, the dye and tracer will follow the lymphatic drainage path towards the sentinel lymph node. Thus enabling this node to be identified by a gamma probe and visually because of the blue dye. The identified lymph nodes are then excised and further examined for pathologies.

The current standard of using a radioactive tracer results in some drawbacks. Most of all, the technique is limited to hospitals outside of the third world, as these often are not able to employ nuclear medicine [8]. Even in developed countries, 40% of all patients do not have access to this technique [9]. Since the half life of the used radioactive isotopes is only six hours, restrictions on time also affect the procedure. Especially since the isotope is administered not by the surgeons, but by the nuclear medicine department of the respective hospital. Furthermore, the exposure of patients to radioisotopes should be avoided whenever possible.

The sentinel lymph node biopsy was developed to produce equivalent outcomes

to those of the axillary lymph node dissection. In this procedure, all axillary lymph nodes are excised to be examined *ex vivo* [10].

2.1.1 Handheld probe

Since the use of radioactive tracers severely limits the applicability of the sentinel lymph node biopsy, the use of another, non-radioactive, tracer could be a suitable alternative. Obviously, the use of a non-radioactive tracer also requires the use of another identifier than the now used gamma probe. For this purpose, a hand held probe has been developed to make use of Differential Magnetometry (DiffMag) to detect SuperParamagnetic Iron Oxide Nanoparticles (SPIONs) [1]. Although the handheld probe and SPaQ are closely related, their respective purposes are different. The sole purpose of the handheld scanner and the SPIONs is to replace the gamma probe and the radioactive tracer respectively in the sentinel lymph node biopsy.

Another, smaller probe is currently being developed to be used in laparoscopic procedures. This is done by separating several components of the current probe; the excitation and detection coil. A large detection coil will be placed underneath the patient, while the detection coil is placed in laparoscopic equipment [11][12].

2.2 SuperParamagnetic Quantifier (SPaQ)

The Superparamagnetic Quantifier uses a combination of AC magnetic fields and DC magnetic field offsets to measure the dM/dH curve of the SuperParamagnetic sample in the sampleholder. dM/dH being the derivative of the magnetization curve, as will be explained in section 2.2.1. The principle of DiffMag will be explained in section 2.2.2.

The height of the measured curve, as well as the DiffMag value, is linearly proportional to the quantity of SPIONs in the sample holder. By using a calibration curve, the exact amount of particles in an unknown sample can thus be determined. While it is beneficial to identify the sentinel lymph nodes *in vivo*, this is not the case for types of cancer where the SLNB is not the clinical standard. For example, in an axillary lymph node dissection (ALND) all axillary lymph nodes are excised to be examined. It then becomes desirable to identify the sentinel lymph node *ex vivo*. SPaQ can be used to determine the SPION content of the lymph nodes and thus identify those most interesting to examine for metastasis.

Besides the possibility of SPaQ to quantify the iron content of lymph nodes directly, it can also be used to qualify the behaviour of the superparamagnetic nanoparticles. The response of different kinds of nanoparticles to the DiffMag protocol executed by SPaQ should be indicative of the response to the hand held probe described in section 2.1.1. While SPaQ measures the entire dM/dH curve, the hand held probe is only able to quantify the amount of SPIONs. SPaQ could thus potentially play a major role in determining the most optimal SPIO nanoparticle to be used in medical procedures such as the sentinel lymph node biopsy.

SPaQ mainly consists of several coils. A large excitation coil is able to produce homogeneous magnetic fields up to 15mT. Within this excitation coil two induction coils can be found. These induction coils measure the field strength, which is altered by the presence of SPIONs. Within the induction coils the sample holder can be placed. This sample holder is large enough to contain a lymph node. The outer coil is placed in a bath of oil for the coils to be able to disseminate heat faster. The

induction coil is connected to a power supply, while the induction coils are connected to several filters before the signal reaches the controlling computer. The SPaQ set-up at the University of Twente can be seen in figure 2.

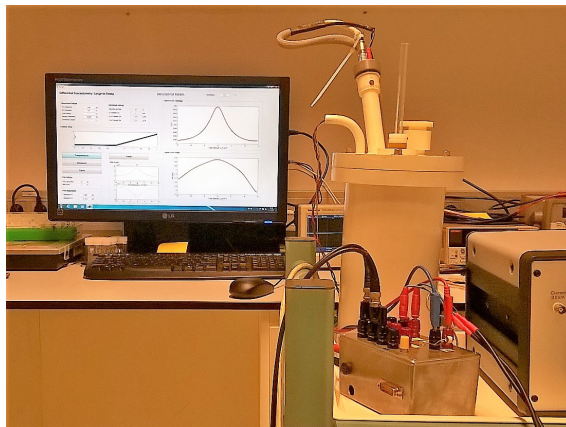


Figure 2: Set-up of the SuperParamagnetic Quantifier at the University of Twente.

The temperature of SPaQ can be controlled either by sending a large current through the excitation coil as to heat up the system. Alternatively, the system can be heated by a thermostat connect to a 20W heater on the bottom of the oil bath. Thermometers are placed in between the excitation and induction coils, and in the oil bath. A third thermometer can be placed in the sample holder. Currently, cooling takes place primarily through convection to the surrounding air.

2.2.1 SuperParamagnetic Iron Oxide Nanoparticles (SPIONs)

The magnetization of a particle represents the response of the magnetic moment to an externally applied magnetic field. In a diamagnetic material, the magnetic moments will oppose the magnetic field, while in a paramagnetic material, the magnetic moments will align with the magnetic field, increasing its strength. Both of these responses are linearly dependent on the field strength. This is not the case for sufficiently small ferromagnets. These particles become superparamagnetic. [3]. The response of diamagnetic and superparamagnetic materials can be seen in figure 3. While most tissue is diamagnetic, SPIONs are, as the name suggests, superparamagnetic. Differential magnetometry makes use of this specific nonlinear behaviour.

Usually, one considers not one single magnetic moment, but rather the sum of all magnetic moments in a sample. If no magnetic field is applied, all magnetic moments will be ordered randomly, such that the sum of all magnetic moments in one direction is zero. The magnetic moment of superparamagnetic particles will attempt to align with an applied field. This will also happen whenever the field is varying over time. In this case however, the frequency of the alternating field becomes more relevant. The alignment of the moments with the field is not instantaneous. Instead, some time passes before the sum of all magnetic moments goes from a disordered state, to the magnetized state and the other way around. The relaxation time is the time constant corresponding to the time it takes for the magnetic moments to go from a magnetized state, to the usual, disordered state. Whenever the magnetic field changes faster than the relaxation time of the particle allows, the magnetization of the sample will lag behind the magnetization of the field.

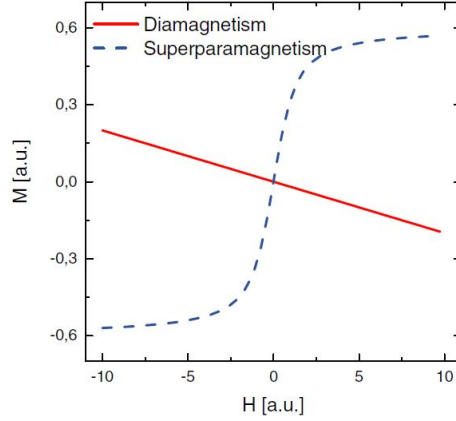


Figure 3: Magnetization due to an applied field for a superparamagnetic nanoparticle and a diamagnetic material [1].

While on the subject of relaxation, a distinction can be made between two relaxation processes; Brownian and Néel relaxation. The magnetic relaxation can be described by a rotation of the magnetic moment vector. This is also where the distinction can be made. For Brownian relaxation, the entire particle rotates, and with it, its magnetic moment. For Néel relaxation, solely the magnetic moment vector rotates, as can be seen in figure 4. Although it is common for one of either relaxation mechanisms to dominate a sample, it is possible for both mechanisms to occur. In this case, the effective relaxation constant is described as follows:

$$\frac{1}{\tau_{eff}} = \frac{1}{\tau_B} + \frac{1}{\tau_N} \quad (1)$$

Particles with a larger core size relax mostly through the Brownian mechanism, while smaller particles relax mostly through Néel relaxation. For particles with a core size about the critical core size, the size where both mechanisms occur, the relaxation time is described by formula 1. Since Brownian relaxation requires the physical rotation of the particle, the obstruction of movement of these particles, will result in a decreased response to externally applied magnetic fields.

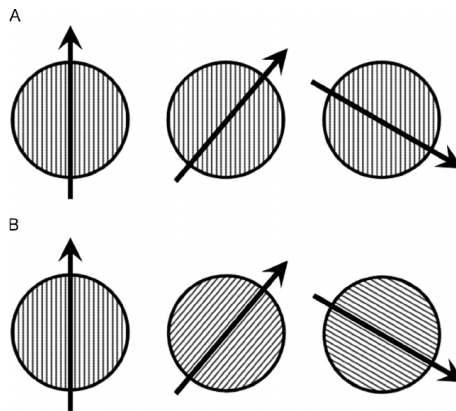


Figure 4: Néel relaxation (A) and Brown relaxation (B) over time [13].

An example of previously described superparamagnetic iron oxide nanoparticles is Resovist. These particles have previously been used as a MRI contrast agent and

have been approved for clinical use. Resovist has a polydisperse core size distribution. Meaning that not all magnetic cores are identical in size. Therefore, neither Néel nor Brown relaxation dominates the sample. Previous studies have shown the effect of immobilizing the particles by freezedrying to illustrate this [3]. Like most SPIONs, the magnetic core is covered by another material. The total diameter being the hydrodynamic size of the particles. Resovist in this case, is usually covered in a biocompatible material like carboxydextran.

2.2.2 Differential magnetometry

SuperParamagnetic Iron Oxide Nanoparticles can be used as a tracer in biomedicine using the non-linear magnetic properties. While in Magnetic Resonance Imaging the high magnetic susceptibility χ is employed to create contrast, differential magnetometry makes use of its non-linear properties. This forms a contrast with the (linear) diamagnetic properties of tissue. As previously illustrated in figure 3. The developed technique resulting in this contrast is called differential magnetometry, or Diffmag.

The SuperParamagnetic Quantifier is able to, but does not primarily use the DiffMag protocol. Instead, another closely related sequence is employed to measure the dM/dH curve. In order to explain this properly, the DiffMag sequency will be explained first. Keeping in mind that this is the mechanism used in the handheld probe, not SPaQ.

The contrast between the non-linear SPIONs and the linear diamagnetic tissue depends on the magnetization M , magnetic susceptibility χ and the magnetic field strength H [3]. Placed in a magnetic field, the total magnetization of a sample containing both the superparamagnetic particles and tissue is simply an addition of the separate magnetizations:

$$M(t) = M_{lin}(t) + M_{spm}(t) \quad (2)$$

Here, the linear and superparamagnetic magnetization are given by equations 3 and 4 respectively. Equation 4 clearly illustrates the non-linear behaviour of the superparamagnetic particles:

$$M_{lin} = \chi H \quad (3)$$

$$M_{spm}(xH) = M_s \left(\coth xH - \frac{1}{xH} \right) \quad (4)$$

Where:

$$xH = \frac{m\mu_0 H}{k_B T} \quad (5)$$

Equation 4 is known as the Langevin function and is extensively used to model the Brownian behaviour of superparamagnetic nanoparticles. To measure the nonlinear magnetization of the sample containing both tissue and SPIONs, an AC excitation field is applied by an excitation coil. This results in a magnetic moment, which in turn results in an induced voltage over a detection coil. This is according to Faraday's law, where the electromagnetic force trough the coil equals the rate of change of magnetic flux trough the coil [14]:

$$\varepsilon = - \frac{d\phi_B}{dt} \quad (6)$$

The induced voltage in the detection coil is proportional to the time derivative of the magnetization in equation 2:

$$U(t) \propto \frac{dM}{dt} \quad (7)$$

To find the effect of the superparamagnetic nanoparticles on the total magnetization of the sample, a sequence of excitation fields is used. This is the concept of differential magnetometry as proposed by Visscher et al. [3], and can be seen in figure 5.

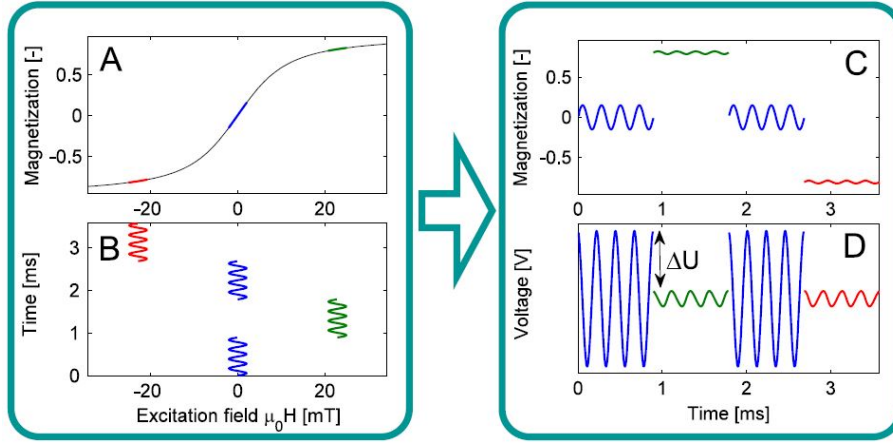


Figure 5: Concept of differential magnetometry [3].

For diffmag, a standard alternating magnetic field is applied and alternated with an offset alternating magnetic field (figure 5B). Due to non-linear magnetization, the induced voltage will be lower for the offset fields, since the slope of the magnetization curve is much lower (figure 5A). The difference in voltage (figure 5D) is then indicative of the amount of the SPIONs in the sample:

$$\Delta\bar{u} = \frac{1}{2}[\Delta\bar{u}_+ + \Delta\bar{u}_-] \quad (8)$$

$\Delta\bar{u}_-$ and $\Delta\bar{u}_+$ are equal to the voltage drop relative to the standard alternating magnetic field for the negative and positive offset fields respectively.

2.2.3 dM/dH curve determination

The SuperParamagnetic Quantifier uses another approach, related to DiffMag, to determine the dM/dH curve of the measured sample. In this approach, an AC field with low amplitude is applied, and added to a DC field, which is gradually increased from the maximum negative amplitude to the maximum positive amplitude. The used sequence can be found in figure 6. The applied DC field can be considered to be the offset field as in the DiffMag sequence. As such, the local magnetic response to the offset field is found for the entire curve. This results in the time derivative of the magnetic moment as a function of the offset field. At the start of each sequence, a constant maximum DC offset is used for a while to eliminate artifacts from the start of the measurement. Therefore, the measurements only starts after this constant field offset. Also, a reference measurement is conducted without sample in the

sample holder. This measurement is subtracted from the measurement with the sample.

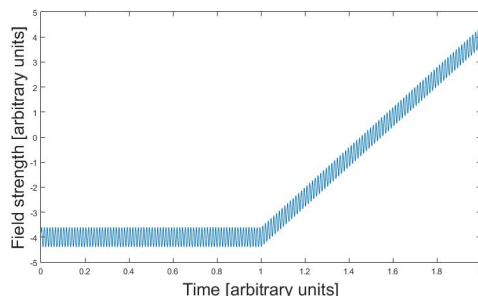


Figure 6: The sequence as used in SPaQ to determine the dM/dH curve.

Currently, the frequency used for the AC field is 2500Hz. This is the frequency as optimized for the hand held probe. The start of the measurement, where the DC offset is kept constant, lasts for one second, which is arbitrarily chosen. The duration of the entire measurement can be varied without affecting other parameters. The amplitude of the AC field is about 1.5mT. Which is not optimized as of yet.

2.2.4 dM/dH curve analysis

The used measurement protocol of SPaQ results in the dM/dH curve of the measured sample. This is the derivative of the magnetization curve. Therefore, integrating the measured curve results in the magnetization curve. As shown in figure 7. This curve can be described by the Langevin function, and is therefore similar to equation 4:

$$L(x) = \coth(x) - \frac{1}{x} \quad (9)$$

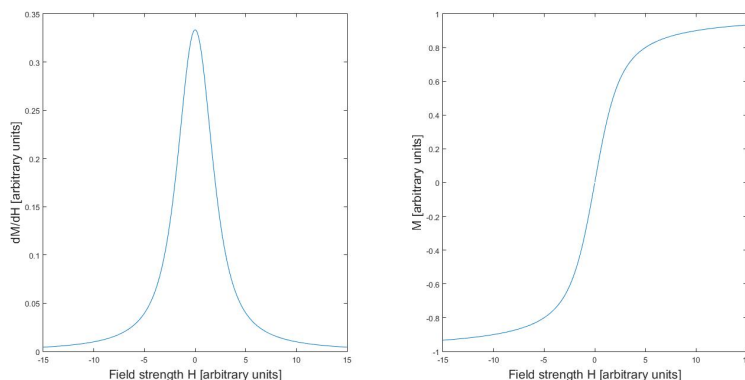


Figure 7: The measured dM/dH curve (left) and the integrated M of H curve (right).

One should keep in mind that not one single magnetization curve exists. This curve is highly dependent on the method used for measuring it. For an alternating field the dynamic magnetization curve is determined, while in a constant field it is the static magnetization curve. SPaQ adds together an AC and DC field. It therefore cannot be considered either static or dynamic. Although SPaQ makes use

of an AC field, this is relatively small in comparison to the DC field it is added to. Therefore, the magnetization curve measured by SPaQ could be considered a hybrid of a static and dynamic magnetization curve. This will become more important when comparing the system to the VSM and MPS. Which result in a static and dynamic magnetization curve respectively.

As SPaQ measures the derivative of the magnetization curve, it is also possible to determine the core size distribution of the measured sample [3]. This is done by fitting it with the derivative of the Langevin function and assuming a log normal distribution of particle sizes.

Furthermore, as mentioned before, the height of the measured peak is linearly proportional to the quantity of nanoparticles in the sample. The creation of a calibration curve will therefore allow one to use SPaQ for the quantification of SPIONs in an unknown sample.

Since SPaQ measures the magnetic response for a large amount of offset fields, it effectively measures the DiffMag value for all of these offset fields. This value can be determined by subtracting the dM/dH value at the offset field from the dM/dH value at $H = 0T$, where the peak of the curve should be:

$$DiffMag(H) = \frac{dM}{dH}(0) - \frac{dM}{dH}(H) \quad (10)$$

This equation holds only true whenever SPaQ does indeed result in the DiffMag values representative for the hand held probe. Hysteresis could cause the maximum of the dM/dH peak to shift to the left or right. Thus creating a difference in DiffMag for negative and positive offsets at identical amplitudes. Whenever this is dependent on the particles, the equation holds true. Whenever hysteresis is caused by SPaQ, it does not.

The hand held probe is solely able to give a single DiffMag value. Since the magnitude of the magnetic field decreases with distance, it is impossible to differentiate between a large amount of SPIONs close to the hand held probe or a small amount nearby. It is therefore desirable to use a particle resulting in large DiffMag values for many field offset values. SPaQ can be used to determine if this is the case for a given particle. The desired dM/dH curve is as high as possible, while also being as narrow as possible. So a high susceptibility and saturation at low fields. This is an application which should be kept in mind while comparing the system to standard methods such as VSM and MPS.

3 Temperature optimization of SPaQ

The derivative of the Langevin curve, as measured by SPaQ is highly dependent on the method of measurement. This will become clear in the comparison to the VSM and MPS. Still, an identical method of measurement should result in identical output curves for the same sample. Specifically, for the analysis as described in section 2.2.4. Currently, this is not the case. Instead, identical measurements only result in nearly identical curves, which are shifted somewhat up or down. For a more accurate comparison of SPaQ to VSM and MPS later on, this inaccuracy will be improved upon in this section. Possible further improvements upon the system can be found in the recommendations, section 9.

3.1 Temperature dependency

As hypothesized in the introduction, the temperature affects the measured curves. Throughout different measurements, the temperature of the system does not stay constant. This is therefore the most likely cause of the observed inconsistencies. This section aims to chart the effect of temperature fluctuations to overcome these later on.

The temperature of the system depends on the inflow and outflow of heat. Besides the obvious heat inflow from the 20W heater on the bottom of the oil bath, heat is transferred through the following mechanisms:

- Heating of the excitation coil due to the resistivity of the coil.
- Heating of the induction coils due to inductive heating.
- Heating of the SPIONs due to the alternating magnetic field.
- Heat transferred through conduction throughout the system.
- Heat transferred through convection from the system to the surrounding air.

Not all of these heating mechanisms affect the output of SPaQ. As will be discussed here and later on in section 3.2.2, where the measurement results illustrate the effect of heating on the system.

The main heating of the system, next to the heater in the oil bath, is caused by the heating of the coils. As an electric current flows through a conductor, it causes the conductor to dissipate heat. This is known as resistive, ohmic or joule heating [15]. The amount of heat dissipated is dependent on the current through the conductor and the resistance of the material according to:

$$P \propto I^2 R \tag{11}$$

To produce the magnetic field in the excitation coil, a current is run through it. This causes the coil to produce heat according to equation 11. This affects the coil wire in several ways. The resistivity ρ of the wire is directly proportional to the temperature. If a voltage is then sent through the wire, this would result in a decreased current. Subsequently, the coil would produce a lower field amplitude. However, this should not affect SPaQ as the field is current driven and a current is sent through the coil. Different temperatures would result in different voltage drops

across the coils (however small). However, this is irrelevant for the field strength, thus not affecting the measurement. More relevant is the expansion of copper due to heating. This could influence the spacing between coil wires and therefore influence the produced field.

The induction coils heat up for the same reason as the excitation coil. Eddy currents are generated by the AC magnetic field through the coil as described by Faraday in equation 6. Alternating magnetic fields through a coil produce a voltage over it. Since it is also a voltage which is measured, the resistivity should not influence the measured curve here either. The expansion of the copper could also play a role here.

Although previously described effects should occur, these are unlikely to be the main cause of the inaccuracies in the measured dM/dH curves as these effects should be negligible. The mutual induction between the excitation and induction coil could be more relevant. This is the voltage generated by the changing magnetic field in the inductance coil. As the copper expands, the geometry of both coils might affect the induced voltage. This is because the mutual inductance is highly dependent on the number of coil turns, area and wire length [15]. The mutual inductance is further dependent on the permeability of the material within the coil. Whenever this permeability is temperature dependent, this would affect the induced voltage too.

The nanoparticles are influenced by temperature too. The particles themselves produce heat whenever exposed to an alternating magnetic field. This is due to the Brownian and Néel relaxation described before. The power dissipated by the particles due to an AC field is given by:

$$P = \pi\mu_0\chi_0H_0^2f\frac{2\pi f\tau_e}{1+(2\pi f\tau_e)^2} \quad (12)$$

This is a property used in the field of hyperthermia, where superparamagnetic particles are used to heat up cancerous tissue as to increase its vulnerability towards chemotherapy and increase cancer cell destruction [16][17][18][19][20].

Since the amplitude of the AC field and the frequency used in SPaQ is low in comparison to the fields used in hyperthermia, this heating of the particles is unlikely to have any effect on the system. Also, the relaxation processes causing the heating are also those enabling SPaQ to measure the dM/dH curves. Not only do the particles produce heat, the magnetization M is influenced by temperature according to equation 5. However, as this temperature parameter is multiplied with the Boltzmann constant in the denominator, this effect could be considered minimal. This effect has previously been measured using MPS [21]. As not the sample temperature, but the system itself heats up in SPaQ, this is unlikely to be the cause.

Although the induction coil and particles heat up themselves, the heat within the system is primarily generated by the current through the excitation coil. This heat is conducted throughout the system to other components. Thus also heating the induction coil, oil bath, air, sample holder and sample. The coil is placed in a bath of oil, to dissipate heat faster. The total heat transfer from and to the system depends mostly on the convection heat transfer rate from the outside of the system to the air. Therefore, the dissipation of heat from the coils is limited by the dissipation of heat to the surrounding air. Currently, no other method of cooling than this convection is possible.

3.2 Determination of temperature dependency

3.2.1 Methods

To find the temperature dependency of SPaQ, identical measurements were conducted, where only the temperature was altered. A Resovist sample with a set amount of iron oxide nanoparticles was used each time and the measurement time was set at one second. It should be noted that these measurements were not conducted in a magnetically shielded room. It was therefore possible for external fields to influence these experiments. These parameters were identical for all of the following experiments. Two series of measurements were conducted. For the first series, the temperature was altered but not kept constant. For the second series, the temperature of the system was kept as constant as possible. This was done using the thermostat coupled to the 20W heater. The thermostat used a negative feedback loop to keep the temperature of the oil bath at $\pm 0.2^\circ C$ of the set temperature. Rather than scaling its output to the desired temperature, it produced either 20W or 0W according to the feedback loop.

Fluctuating temperature measurements

For the first series of measurements, the temperature was set to $25^\circ C$, $30^\circ C$, $38^\circ C$ and $45^\circ C$ respectively. As each of these temperatures was reached, five measurements were conducted subsequently in rapid succession. This did not allow the system to cool down in between measurements. The temperatures of the oil bath and the coils were recorded both before and after each measurement. These can be found in table 2 in appendix A. Here T_{mat} represents the temperature of the coils, while T_{heater} represents the temperature of the oil bath.

Constant temperature measurements

For the second series of measurements, the heater was used similarly to reach $25^\circ C$, $28^\circ C$ and $31^\circ C$. These values were chosen since these are above room temperature, such that fluctuation of the room temperature would not affect the system significantly. Each measurement was preceded by a waiting period of a couple of hours. This allowed the system to reach a thermal equilibrium and thus be at a more constant temperature than for the previously conducted measurements. The highest temperature, $31^\circ C$ was chosen as this was the thermal equilibrium reached for a constant heat transfer rate of 20W. This being the maximum of the used heater. This time the temperature of the sample holder at the start of each measurement was recorded too, to determine the temperature distribution of the system at thermal equilibrium.

Sample holder size effect

As the sample holder is large enough to fit a lymph node, the smaller sample tube containing Resovist placed in the sample holder of SPaQ is not fixed at one position. It is therefore possible for the sample to be placed in different positions each measurement. Although this is not related to temperature fluctuations, this could influence the dM/dH curve. To find the influence of different positions of the sample in the sample holder, multiple measurements are conducted with identical placements of the sample. This is done by securing the sample in place by a roll

of paper inside the larger sample holder. This effectively decreased the size of the sample holder.

3.2.2 Results and discussion

Since only one sample was used, this section will focus on the comparison between measurements, rather than on the analysis of measured dM/dH curves. The results of previously described measurements will be displayed as well as discussed here.

Fluctuating temperature results

The first series of measurements resulted in numerous, inconsistent curves. This illustrates the problem as described in the introduction. This can be seen in figure 8. Each curve is labeled with its respective starting temperature as indicated by the thermometer in between the coils. An overview of all measured temperatures can be found in table 2 in appendix A.

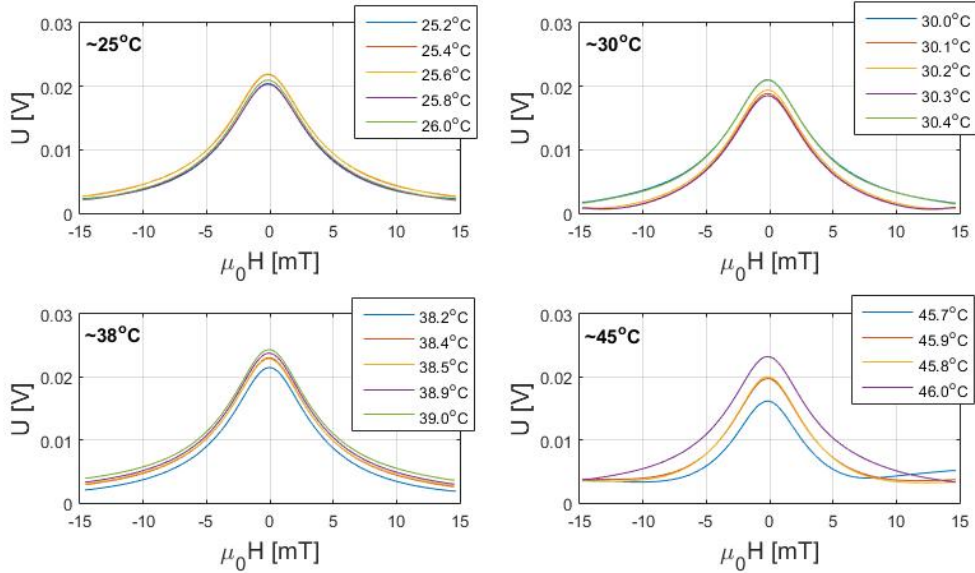


Figure 8: Measured output curves for identical measurements at different starting temperatures. In these measurements, the temperature was not kept constant throughout the measurement and system.

The measured temperatures indicate not only that the temperature distribution throughout SPaQ is far from homogeneous, but also that each measurement the coils heat up about 0.1°C . This because each subsequent measurement is started at a somewhat higher temperature. As these measurements last only one second, this means the heating of the coils is a rapid process.

The results as displayed in figure 8 show that each measured curve contains some drift. Furthermore, the shape of each curve is different. According to equation 10, this also means the DiffMag values for different offsets will be different.

Constant temperature results

Figure 9 shows the results of the measurements where the temperature was kept con-

stant. Additionally, all measured temperatures can be found in table 3 in appendix A. Also, figure 9D, shows the DiffMag values as determined by each measurement. From figure 9A - C clearly follows that the drift as measured before is still present. The determined DiffMag values however, show that the shape of the measurement remains largely identical up to 10mT. This is the case for all measurements across temperatures. This leads to the conclusion that the temperature is irrelevant regarding DiffMag, however, temperature fluctuation are not. Therefore, keeping the system at a constant temperature will result in more reproducible results.

The measured drift does seem dependent on temperature, as figure 10 illustrates. The maximum height of measurements at constant temperature increases for higher temperatures. Also, at $25^{\circ}C$ the measured curves seem more constant. However, the amount of measurements does not allow conclusions to be drawn from this observation.

For constant temperatures, the shape of the curve, and thus the DiffMag values, remain identical only up to 10mT. SPaQ can therefore only be considered reliable up to this point. Minor differences between curves beyond 10mT can be explained by the fact that the largest currents are sent trough the coil at this point. For some measurements though, the dM/dH curve increases in amplitude beyond 10mT, even though it should decrease or remain constant according to its superparamagnetic properties. Seemingly, the curve is reversed at this point. Probably due to the fact that an absolute value is used to plot the curve. This is required since the measured voltage consists of a real and imaginary part. Rather than measuring only up to 10mT, data beyond this point is discarded after each measurement. This because the effects of measuring up to smaller field strengths has not yet been explored.

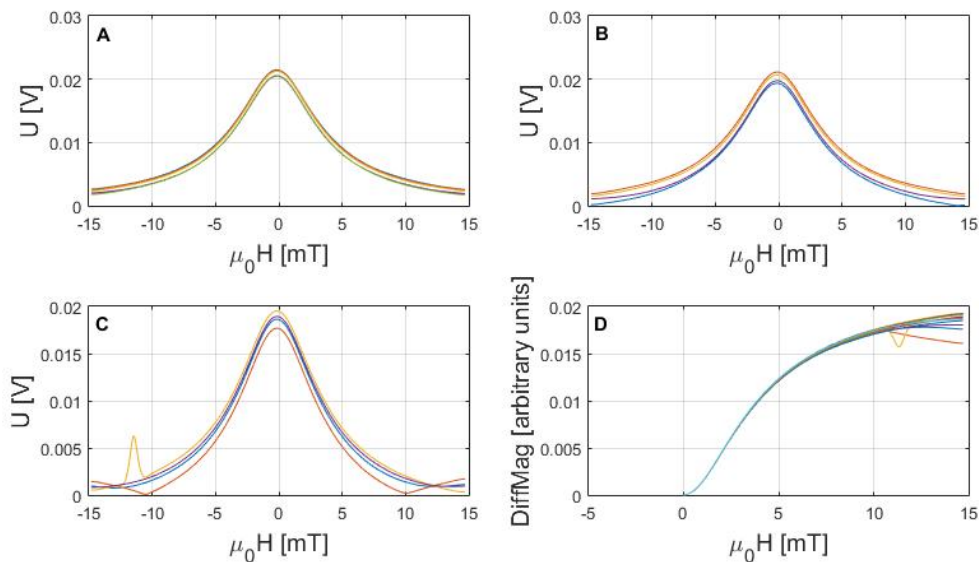


Figure 9: Measured output curves for identical measurements at $25^{\circ}C$ (A); $28^{\circ}C$ (B); $31^{\circ}C$ (C) and the DiffMag values of these measurements (D).

Even at constant temperature, drift remains. Only some of it could depend on temperature as indicated by figure 10. The fact that the shape remains identical

throughout each measurement, results in only a couple of explanations for this observation. Clearly a constant value is added to, or subtracted from each measurement. Alterations of the field would result in a different shapes of the dM/dH curves, since the SPIONs respond differently to other field strengths. The offset can therefore only be caused beyond the detection coil, within the electronics of the system. Otherwise, the found dM/dH curve shape would not be identical each measurement. The most likely cause of the drift is the reference measurement executed before each measurement. This empty coil reference is subtracted from the measurement where the sample holder contains a sample. This zero coil measurement usually results in a constant dM/dH signal for varying fields. This could therefore be treated as a constant value added to the measured data. Obviously, this reference should remain the same during the reference measurement and the measurement with the sample. If this were to change, this would result in a constant offset value, as is the case now. Solutions for this problem will be discussed in the recommendations, section 9.

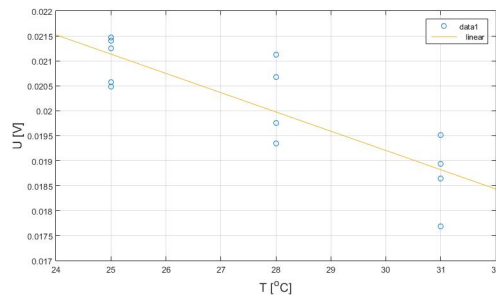


Figure 10: The maxima of all measurements for the constant temperatures at which they are measured. Also shown is a linear fit of the plotted data.

Sample holder size effects

Securing the sample in place rather than allowing it to move somewhat in the sample holder did not result in a visible impact on the measured results. Similar results to those where the temperature was kept constant were obtained. For further experiments it was therefore neglected to secure the sample more tightly.

3.3 Data compensation for fit

Even though reproducible DiffMag values can simply be achieved by keeping the SPaQ at a constant temperature, to achieve a constant drift for every measurement, other approaches are required. Probable solutions regarding this problem are discussed in the recommendations, section 9. This section offers a proof of concept for a workaround. In this approach, the vertical offsets as measured are compensated during post processing of the measured data. Although this method offers limited reliability, as it introduces an error in the processed data, it does result in more reproducible outcomes of the SPaQ.

The workaround uses the fact that, although output curves are plotted at different heights, the curve shapes are identical up to 10mT. Furthermore, it uses the fact that the measured dM/dH curves should be zero beyond the saturation field strength. Since SPaQ is only able to measure dM/dH in low fields, this field strength

is usually not achieved. Therefore, the measured data is fitted and extrapolated to estimate this value. The used approach is illustrated in figure 11.

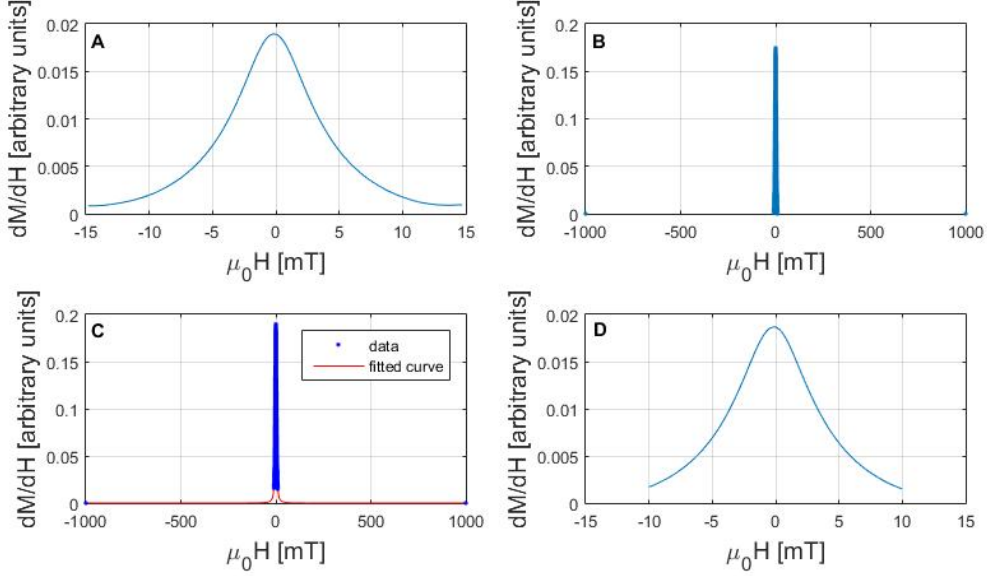


Figure 11: Procedure for fit compensation of the measured dM/dH curves by SPaQ; the measured data (A); deletion of all data beyond $\pm 10mT$ and the addition of data points at $-1000mT$ and $1000mT$ (B); fit with the derivative of the Langevin function for different heights of the original data, while the added data points remain unaltered (C); data compensated for fit (D).

First, all data beyond $10mT$ is discarded, as this has shown to be unreliable. Then, two additional data points are "added". Since superparamagnetic particles are completely saturated at higher fields, dM/dH should be zero. This is why at $-1000mT$ and $1000mT$, dM/dH is set at zero. $1000mT$ is chosen since this should be sufficiently far into saturation. Now, this altered dataset is fitted using the derivative of the Langevin function. This is done for multiple heights of the data, with the exception of the added data points, which remain zero. This results in the best fit for a certain height. Which is determined using the sum of the squared residual. The found height should be appropriate height for the measured data. For those curves with an identical shape, this naturally should result in identical heights too.

As mentioned before, the data is fitted for the derivative of the Langevin function as given in equation 9. This derivative is equal to:

$$\frac{dL}{dx} = \frac{1}{x^2} - csch^2(x) \quad (13)$$

One should note that this equation is only an approximation of the Brownian behaviour of SPIONs. This does introduce an error in the compensated data for this fit. However, since the fit is solely used to approximate the appropriate height of the curve, this is not an unreasonable approximation. The Magnetic Detection & Imaging group has previously developed a model combining both Néel and Brown relaxation. However, the amount of variables and therefore runtime required for this

model to be used as fit, render it unusable for this purpose. The fit function derived from equation 13 only relies on two parameters to be fitted:

$$Fit = \frac{1}{a * (x - b)^2} - a * csch^2(a * (x - b)) \quad (14)$$

Here x is equal to the field strength H , while a and b are the parameters to be fitted. As the Langevin function describes the behaviour of a single SPION, a more accurate fit function would be a sum of equation 14. However, this would result in an increase in fitting parameters, therefore increasing the required runtime.

For post processing of the measured data, MATLAB was used. The default fit function and its default fit settings were used to fit the data. Also, each fitting was preceded by a multiplication of all data by an appropriate multiple of ten. This because the used model in equation 14 is not applicable for too low values of dL/dx . After each fit, the data was divided by the same scaling factor, to compensate for this element of fitting.

Figure 12 shows that the measured data of the SPaQ does become more reproducible because of the previously described data fitting. Of course, the reliability of the determined height depends on the accuracy of the fit. As the Langevin function only approximates Brownian behaviour and only two fitting parameters were used, this does result in an error. However, as the fit is solely used for the determination of the proper height, the true effect of this error will only become apparent whenever this height becomes more relevant. This is the case whenever the curve is integrated to find the M curve. Therefore, the height of the compensated curves should be treated with some criticism. The curve height is irrelevant for the quantification of SPIONs, as the DiffMag approach used for this is not dependent on the height of the dM/dH curve, but solely its shape.

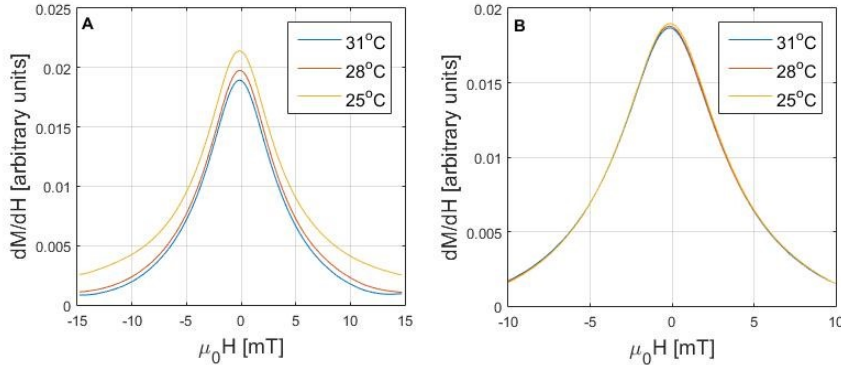


Figure 12: Corrected data for the Langevin fit; the unaltered data for three measurements at different constant temperatures (A); the same data compensated for the fit (B). As the data beyond 10mT is not used for the fitting, it is not displayed in the compensated plot.

Finally, it was determined that the appropriate waiting time for SPaQ to be able to reach thermal equilibrium is about half an hour. This is sufficient whenever only one measurement of one second has been conducted at 31°C. To reach thermal equilibrium initially, longer periods are required. For this reason, for further measurements, the system was kept at 31°C by continuously heating the system with

the 20W heater. In between each measurement, the system was kept idle for thirty minutes.

4 SPaQ compared to Vibrating Sample Magnetometry

4.1 Vibrating Sample Magnetometer

Currently, the vibrating sample magnetometer (VSM) can be considered the standard method for the determination of magnetization curves. Rather than measuring the derivative of the magnetic moment, M_{total} is measured directly. In the VSM, a static magnetic field is used. Rather than alternating the field, as in SPaQ and MPS, the sample is vibrated. The static field results in a magnetization of the magnetic particles within the sample. As the sample is vibrated, this induces a voltage across the detection coils [22]. By gradually changing the amplitude of the static magnetic field, the entire magnetization curve can be determined.

Obviously, equation 2 to 5 still apply. However, one should note that the VSM results in the static magnetization curve. Since a static field is used, there is barely any Brownian or Néel relaxation due to rapid changes of the field. One should note that the magnetic moments do relax whenever the static field amplitude is altered. Although these alteration should be slow enough for no lag to occur. This lack of relaxation should result in a different magnetization curve than that determined by SPaQ. The measured effect is fundamentally different than that measured in SPaQ or MPS, which will be explained in section 5.

As a VSM is able to apply fields up to 9T, the use of superconducting coils and therefore, liquid helium, is required [8]. 4T fields have previously been used to quantify SPIO nanoparticles in a sample [4]. Because of the use of these large fields, SPIONs are usually driven far into saturation. Usually, the vibration amplitude is about 2mm, while the used frequency is about 40Hz.

Although the SPIONs in the sample are driven into saturation at high field amplitudes, a linear trend often remains. This due to diamagnetic or paramagnetic behaviour of the sample holder. Since only the superparamagnetic behaviour is interesting for now, this linear trend should be removed. This can either be done by subtracting a reference measurement, or by removing a linear trend [23].

4.2 Sample preparation

In order to compare the VSM to SPaQ, several samples of Resovist are measured in both systems. For the VSM, some sample preparation is required. This system only allows for small sample sizes. Therefore, $15\mu L$ sample tubes have been used. These are closed using a rubber cork and parafilm, as the VSM vibrates the sample at approximately 40Hz. This is also why it is somewhat inaccurate to measure liquid samples. Vibrations could cause the SPIONs to be shaken trough the sample tube, therefore affecting the measurement. This is why both liquid samples have been prepared, as well as several immobilized samples.

For this purpose, some Resovist was gelled in a dextran hydrogel. To achieve this gel, Dextran-Tyramine, Ferucarbotran and Hydrogen peroxide were added to a set amount of Resovist, resulting in a more viscous hydrogel containing a certain quantity of Resovist [24]. Theoretically, this should result in the SPIONs being secured in between the cross links of the hydrogel. The degree of immobilization could be determined by measuring fully immobilized samples containing identical

SPION quantities. Comparing the resulting dM/dH curve using SPaQ or MPS, the degree of immobilization should become clear. The complete immobilization of SPIONs can be achieved by freeze-drying.

For the purpose of comparison, Three concentration of Resovist in Dextran gel have been prepared. Each of a total volume of $15\mu L$ and concentrations of $1\mu L$, $2\mu L$ and $3\mu L$ Resovist respectively. Furthermore, four samples of liquid Resovist have been prepared. Three with identical concentrations to the Dextran samples and one containing the maximum amount of $15\mu L$ Resovist. Additionally, some reference samples have been prepared: a sample tube containing solely Dextran gel, an empty sample tube with cork and parafilm, and an empty sample tube with parafilm.

4.3 Methods

All samples are measured with both SPaQ and the VSM. For both systems, default settings have been used in order to compare SPaQ to the standard method. For SPaQ this means that up to a field strength of $15mT$ is measured. The used frequency is $2500Hz$, the used amplitude $1.5mT$ and measurement length one second. Or: identical settings to those used in section 3.

Default settings for the vibrating sample magnetometer include a $40Hz$ vibrating frequency and a $2mm$ vibration amplitude. As $4T$ has previously been used to quantify SPIONs in a sample, this was used once again. Since SPaQ is only able to measure accurately up to $10mT$, the low field amplitudes are more relevant regarding the comparison than the high fields. Therefore, only for the field amplitudes of $-500mT$ to $500mT$ the maximum amount of data points were gathered, by slowly changing the field amplitude. For all field amplitudes above this, the field increments were increased to reduce measurement time. Therefore also reducing the amount of measurement points at these sections of the curve. This brought the total measurement time to about half an hour. A continuous measurement approach was employed, meaning that the field amplitude was increased gradually. The magnetization curve is determined in two directions, so for field variations from $-4T$ to $4T$ and from $4T$ to $-4T$.

All measurements conducted with SPaQ have been compensated using the Langevin fit described in 3.3. For each VSM measurement a linear trend was subtracted as determined by the linear behaviour at saturation amplitudes. Although the linear trend is often removed by subtracting the reference measurement, this would result in inconsistent results in this case. Not all resulting M curves contained an identical linear trend, thus rendering this approach unusable.

4.4 Results and discussion

Figure 13 display the results SPaQ yielded for the prepared samples using the measurement settings as described in the previous section.

A couple of observations can be made from figure 13A. First of all, the maximum of each curve is not found at an offset field of zero Tesla. Instead, it is found somewhat to the left. This indicates that some hysteresis is present, even though this should not be the case for super paramagnetic particles. Measurements where the DC field offset was increased in the opposite direction, so from $15mT$ to $-15mT$, resulted in a shift of the peak to the right of the zero offset. Thus confirming the

occurrence of hysteresis. This could be due to the passing of the expiration date of the Resovist, causing the particles to cluster together.

What else should be noted, it that the maximum peak height for each concentration is higher for Resovist samples solved in water than for those gelled in Dextran. This indicates that the hydrogel in fact does immobilize some of the particles, thereby preventing Brownian relaxation.

Figure 13B shows the DiffMag value for the range of measured offset fields for each measurement. This shows that the DiffMag value is a reasonable indication of the quantity of SPIONs contained in the sample. This is further illustrated by table 1. Displaying the DiffMag value at a 5mT offset. Although based on these values one can make a clear distinction between each quantity, the DiffMag values do not scale linearly with the quantity of iron in the sample, as it should. This inaccuracy could be due to pipetting errors, but also due to inaccuracies within the system. Especially since each sample only contains a limited amount of iron. Only 28 grams per μL .

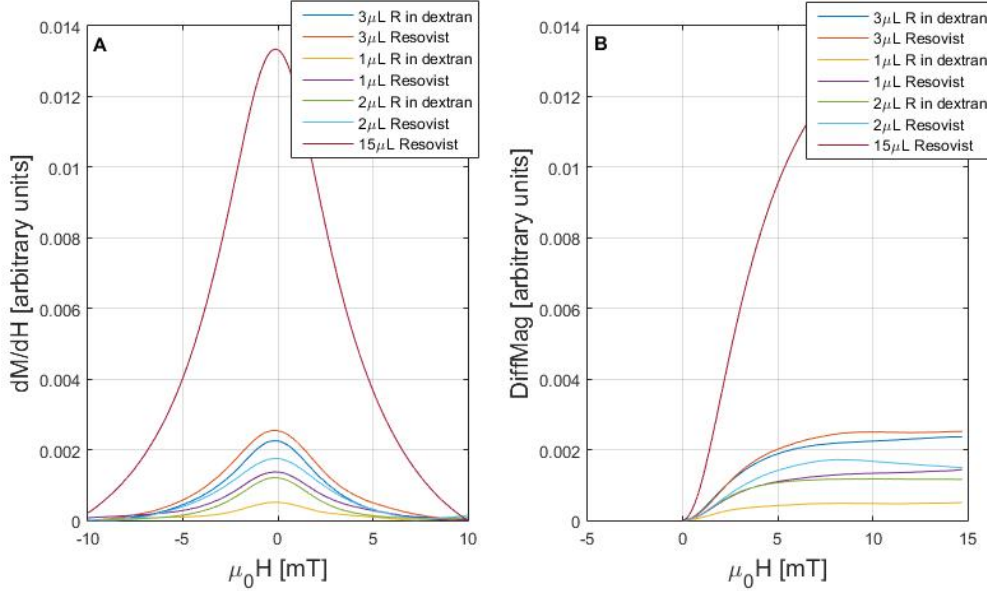


Figure 13: dM/dH curves as measured by SPaQ for liquid and gelled Resovist samples (A) and the DiffMag values associated with this curve (B).

Table 1: DiffMag values at an offset of 5mT as measured by SPaQ and saturation magnetization as measured by the VSM.

Sample	DiffMag [arbitrary units]	Saturation magnetization [Am^2]
1 μL R in dextran	0.0004	1.88
2 μL R in dextran	0.0010	4.43
3 μL R in dextran	0.0019	6.95
1 μL Resovist	0.0011	2.82
2 μL Resovist	0.0014	3.76
3 μL Resovist	0.0020	6.16
15 μL Resovist	0.0095	31.68

The resulting magnetization curves of the VSM are displayed in figure 14. Figure 14A-C show the magnetization curves as measured, while 14D shows three selected curves for the low field amplitudes SPaQ is able to measure.

The saturation amplitude should be indicative of the quantity of SPIONs in the sample. For the Dextran hydrogel samples, this is a nearly linear trend, as it should be. This is further illustrated in table 1. There is some error, however, this could be explained by pipetting errors. For the liquid Resovist samples the saturation magnetization does indicate a higher or lower quantity of iron, however, this is not linear. This is as expected, because of the vibration of the sample. Movement of the nanoparticles could therefore easily affect the measurement. Comparison of the hydrogel and liquid samples regarding quantification is not possible, due to the nonlinear quantification curve of the liquid samples.

The quantification curve resulting from the SPaQ cannot be considered completely linear either. As the used Resovist samples were past their expiration date, clusters might have formed. This could result in hysteresis, and possibly this non-linear quantification curve. Hysteresis shifts the measured dM/dH curve to the left, thus affecting the DiffMag values as given by equation 10. This would be the case, as the shown DiffMag curves consist of the average between the negative and positive offsets.

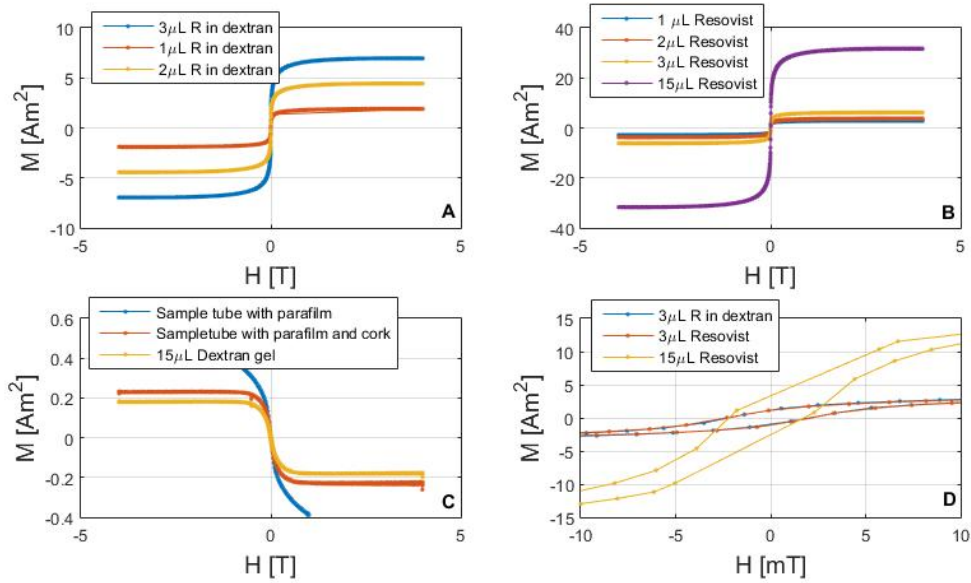


Figure 14: M curve results of the vibrating sample magnetometer; M curves Resovist samples in a Dextran hydrogel (A); M curves liquid Resovist samples (B); M curves of reference samples (C); Three selected M curves for low field amplitudes (D).

The M curves of three reference samples, shows some odd magnetic behaviour of the used rubber cork. The empty sample tube with parafilm M curve indicates mostly diamagnetic behaviour, except for a small deviation from linear behaviour near the end of the curve. As the curve is not measured further, this cannot be explored further at the moment. At low fields, the reference sample can be considered to be diamagnetic. These are the field amplitudes relevant for the comparison with SPaQ. Therefore, this observation will not be explored further. Both reference

samples containing the used rubber cork show diamagnetic behaviour for low fields, while at high fields saturation occurs. In all reference samples, some hysteresis occurs. As the magnetization of the reference samples is at least a factor 10 smaller than the measured samples, this should not affect the displayed results too much. Since the linear trend in the reference samples is not identical to that of all the measured samples, a delinearization algorithm is used to plot all M curves.

A number of observations can be made from figure 14D. First, most obvious is the occurrence of hysteresis. Although this is not initially clear from the full M curves, in all samples hysteresis was present. It is unclear if this is an effect of the sample tube, cork and parafilm, since these reference samples also displayed some hysteresis. As a continuous measurement approach was used, the alterations of the field could also be considered to be too fast. Measurements with incremental changes of the static field could potentially remove this hysteresis, as the field is then allowed to stabilize. As this takes time, the relaxation due to field changes is allowed to relax longer and is therefore less able to lag behind.

Another observation is the small amount of data points in the low field. Although the highest sampling rate was selected, each mT only about one data point is measured. This even becomes clear by figure 14A-C, where each data point can be distinguished at low fields amplitudes.

Moreover, at low fields the liquid Resovist and Dextran sample cannot be distinguished. Although the saturation magnetization is different, both shown hysteresis curves are identical. This suggests the effects of using a liquid sample only become more apparent at higher field strengths. Alternatively, one could argue that the limited amount of data points results in an inaccuracy.

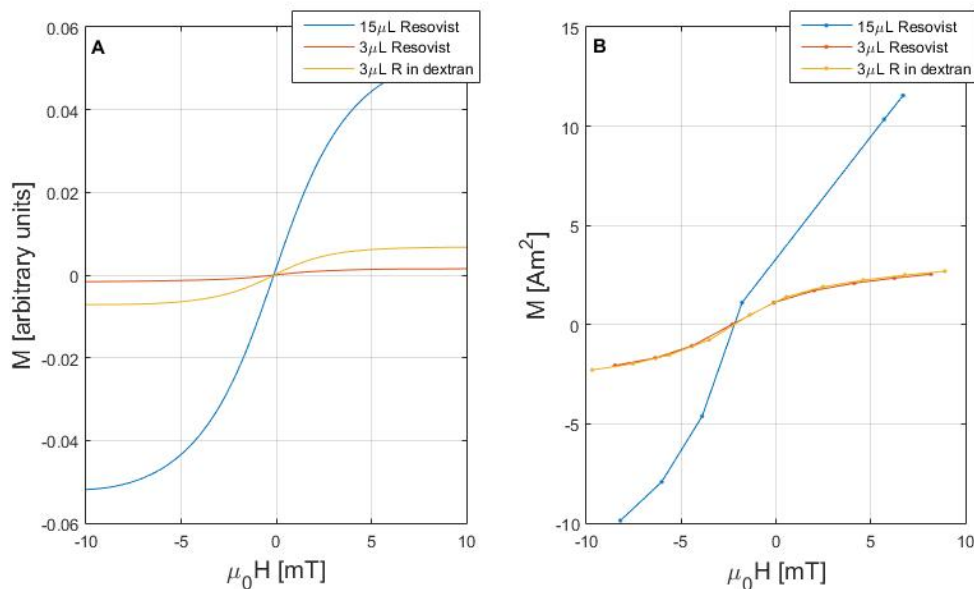


Figure 15: Side by side comparison of M curves generated by integrating SPaQ measurement results (A) and M curves determined by vibrating sample magnetometry.

To directly compare the results from both SPaQ and the VSM, either the M curve needs to be differentiated, or the dM/dH curve integrated. Both approaches would result in some error, as numerical differentiation of the VSM's M curves would

require the data to be interpolated before differentiation. This because of the low amount of data points. In this case, the accuracy of the determined dM/dH curve would depend on the accuracy of this fit. Although the reliability of the integrated SPaQ curves highly depends on the fit compensation for height, this approach has been chosen. Keeping in mind that this acquired result depends on this fit, both results are compared in figure 15. As SPaQ only measures half of the magnetization curve, only this half is plotted for the VSM curves too. This half being the data points measured for the magnetic field sweep from the negative maximum amplitude to the positive maximum amplitude.

Similarities between both the M curves from the SPaQ and VSM include the indication of hysteresis. For neither systems, the M curves pass through zero. Clearly, the M curves measured by VSM cross the zero magnetization axis at a higher field than those measured by SPaQ. In the dM/dH domain this would thus result in a higher offset of the peak to the left. Also, both systems show the $3\mu L$ Resovist samples heading toward saturation near the edges of the plot window. Of course, as this is highly dependent on the height of the dM/dH curve, no further conclusions can be drawn here.

The use of arbitrary units does not allow all curves to be plotted simultaneously. Although normalization could solve this, the limited amount of data points does not allow for proper normalization of the VSM data. Regardless, one can conclude the measured curves are far from identical. This is because the vibrating sample magnetometer is unable to differentiate between a liquid and gelated Resovist sample at low fields. As SPaQ is able to do so, the magnetization curves as measured by SPaQ and the VSM are not identical.

The differences in magnetization curves are as expected. While the VSM measures a static curve, SPaQ measures a more dynamic, curve. Note that this curve is not fully dynamic either, as it is in the Magnetic Particle Spectrometer. A comparison regarding the intended application of the SuperParamagnetic Quantifier will be made in the discussion, section 7.

5 SPaQ compared to Magnetic Particle Spectroscopy

5.1 Magnetic Particle Susceptibility

Magnetic Particle Imaging (MPI) is a medical imaging technique where the distributions of SPIONs is determined in space. Like in Magnetic Resonance Imaging (but not identical to), gradients in magnetic fields are used to create a tomographic image. In MPI, the frequency response of superparamagnetic particles to varying magnetic fields is used to create the image [6][5].

Magnetic Particle Spectroscopy is used to determine the suitability of SPIONs for use in MPI. As in SPaQ, the dM/dH curve is measured. Additionally, the harmonic signal spectrum can be determined, as this is more relevant regarding MPI.

Figure 16 illustrates the principle of MPS. A large alternating magnetic field is applied. This drives the magnetization of a sample hence and forth into saturation (or as far as the field amplitude allows). This results in a changing magnetic moment over time, which induces a voltage in the detection coil. This voltage represents the dM/dt curve according to equation 7. This can easily be converted to dM/dH and will therefore often be treated similarly. The frequency of the excitation signal determines the number of times the dM/dH curve is measured. The positive dM/dt signals as shown in figure 16d are the curves measured from a negative amplitude to the positive amplitude. The negative dM/dt signals are measured from the positive amplitude to the negative amplitude. By averaging these signals, the dM/dH curve can be reconstructed.

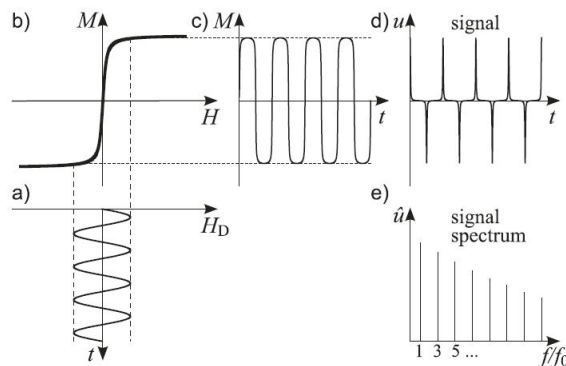


Figure 16: Principle of Magnetic Particle Spectroscopy; the excitation signal drives an alternating magnetic field (a); the magnetic moment of SPIONs follow this field according to the magnetization curve (b); the sinusoidal excitation signal results in a changed magnetic moment over time (c); the derivative of this magnetization is measured as a voltage (d); taking the Fourier transform of this signal results in the harmonic signal spectrum (e) [6].

Integration of the measured dM/dH curve results in the dynamic magnetization curve. Since MPS is used to determine a particle's suitability for MPI, this is usually neglected. Instead, the Fourier transform is used to transform the time signal to the harmonic signal spectrum, as seen in figure 16e. A basic rule of thumb is; more harmonics mean the particle is more suited for MPI.

Although similar, the physical phenomena measured by SPaQ and MPS are not identical. The magnetic particle spectrometer depends on much more relaxation

than SPaQ. This because no DC offset is applied, while the AC amplitudes are much higher for the MPS. Therefore, in magnetic particle spectroscopy the dynamic dM/dH curve is measured, rather than the static dM/dH curve. This will be discussed further in section 5.3, where this is illustrated by conducted experiments.

5.2 Methods

Similar to the comparison with the vibrating sample magnetometer, several samples have been prepared to be measured with both the SPaQ and the MPS.

As the magnetic particle spectrometer requires samples to be contained in a micro titer well, these have been used for all measurements. The micro titer wells all contained a volume of $150\mu L$ in total. Resovist samples with varying concentrations were prepared; 100% Resovist, 10% Resovist, 1% Resovist, 0.1% Resovist and 0% Resovist (demiwater) as reference. Additionally, a freeze dried sample containing an unknown amount of iron particles was prepared.

All measurements have been performed in SPaQ with identical settings to those used in section 4.3. Multiple settings have been used in the MPS experiments. Only the frequency, field amplitude and number of averages were changed. Other parameters remained constant for all measurements. The length of each measurement is dependent on the number of averages, as each average took 0.1 seconds.

Each period of the excitation signal results in a separate dM/dH curve. All the dM/dH curves found in 0.1 second are averaged. Therefore, the number of curves this average consists of, is dependent on the frequency. Whenever a certain amount of averages is selected, this results in a number of averaged dM/dH curves. This is once again averaged to find the final dM/dH curve. Effectively, the Signal to Noise Ratio (SNR) is reduced by increasing the measurement time to average more signals. The required amount of averages was determined by empirical observations. The minimum amount of averages resulting in a smooth output curve was selected.

Five averages have been used to measure at 1kHz, 2.5kHz and 10kHz for an amplitude of 25mT. at 2.5kHz, additional experiments have been conducted with an amplitude of 10mT. For these measurements 10 averages were taken.

For direct comparison with the SPaQ, the frequency of 2.5kHz and amplitude of 10mT was chosen. 10mT was used as this is the field where the SPaQ outputs reproducible results. Experiments with 25mT were conducted as this is the maximum attainable field strength for the spectrometer. 10kHz has previously been used for MPS [25]. At frequencies above 25kHz tissue heating would occur, as quantified by the specific absorption rate (SAR). At low frequencies peripheral nerve stimulation (PNS) could occur [5]. As MPS is designed to optimize SPIONS for MPI, these factors are often taken into account.

5.3 Results and discussion

Similar results as those measured in section 4.4 are found for the measurements made with SPaQ. These can be found in figure 17. As was the case for previous measurements, an offset to the left indicates the presence of hysteresis. The dM/dH curve for the freeze-dried sample behaves similarly, but no conclusions regarding the quantity can be drawn, as the quantity of iron within this only freeze-dried sample is unknown. Also, the height of the peaks are linearly dependent on the amount of

SPIONs in the sample, as is the DiffMag value. One should note that the smallest sample of containing $0.15\mu\text{L}$ Resovist could not be detected by the SPaQ. Like the demiwater measurement, this only shows a linear curve, indicative of diamagnetic behaviour as expected from water.

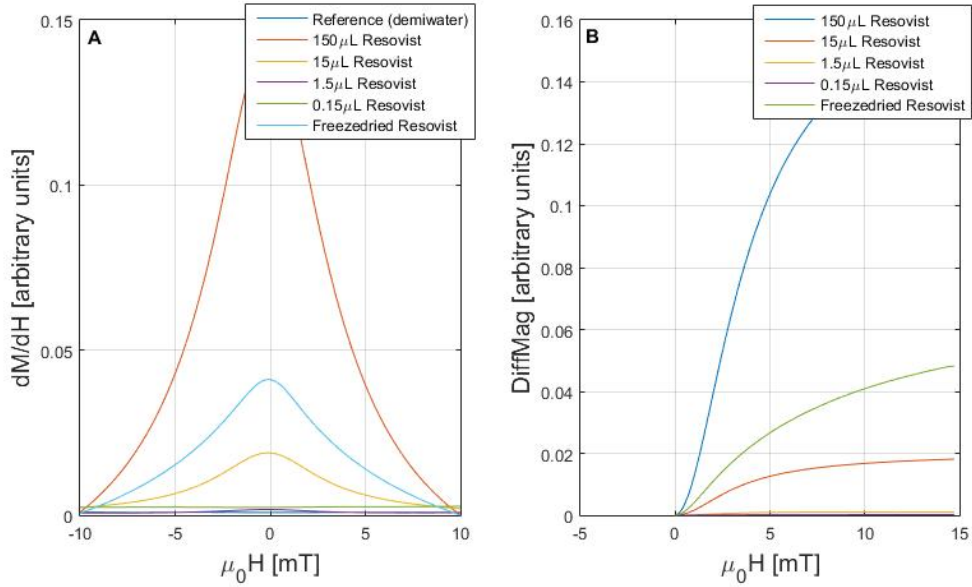


Figure 17: dM/dH curves as determined by the SPaQ for multiple concentrations of Resovist and freeze-dried Resovist.

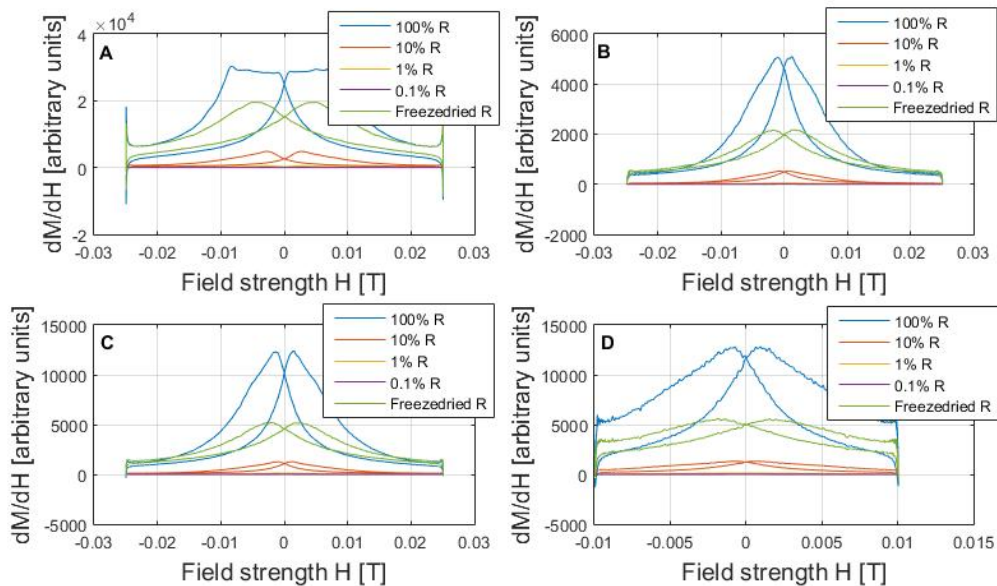


Figure 18: dM/dH curves measured by MPS for different frequencies, amplitudes and number of averages; 10kHz, 25mT, 5avg (A); 1kHz, 25mT, 5avg (B); 2.5kHz, 25mT, 5avg (C); 2.5kHz, 10mT, 10avg (D).

The same qualitative observations can be made for the MPS measurements. For these, the resulting dM/dH curves are plotted in figure 18. As the MPS measures in two direction, two peaks are shown, also indicating hysteresis. For quantification of SPIONs in the samples, the same linear dependence on the amount of Resovist is shown for all measurement settings. As was the case for SPaQ, $0.15\mu L$ Resovist did not result in a measurable signal. Although arbitrary units are used, the use of a higher frequency increases the measured amplitude. This is as expected, as the signal should increase for higher frequencies.

What should be observed, is the height of the freeze-dried dM/dH curve peak. This is, relative to the other peaks, the same for SPaQ and MPS. The maximum of the dM/dH curve of the freeze-dried sample lies in between the maxima of the dM/dH curves of the samples containing $150\mu L$ and $15\mu L$ Resovist. Since Brownian relaxation is obstructed in the freeze-dried sample, this shows that both systems rely similarly on Brownian and Néel relaxation. Because an alternating magnetic field is used in both systems, the particle's magnetic moments are continuously relaxing. Either through Brownian or Néel relaxation. The obstruction of Brownian relaxation would result in a lower dM/dH magnitude, as less magnetization is possible. Therefore, similar peak heights for both systems in a freeze-dried sample indicate a similar dependency on Brownian and Néel relaxation.

Another noticeable aspect is the flattened peaks for the largest measured sample at 10kHz. This is caused by the limited capacity of the used data acquisition card. Furthermore, in figure 18 large peaks can be observed at the highest magnetic field amplitudes. This is an artifact resulting from a division by zero.

Figure 19 displays the dependence of the measured dynamic magnetization curve by the MPS on frequency and field amplitude. This is where the distinction between the SuperParamagnetic Quantifier and the Magnetic Particle Spectrometer can be made.

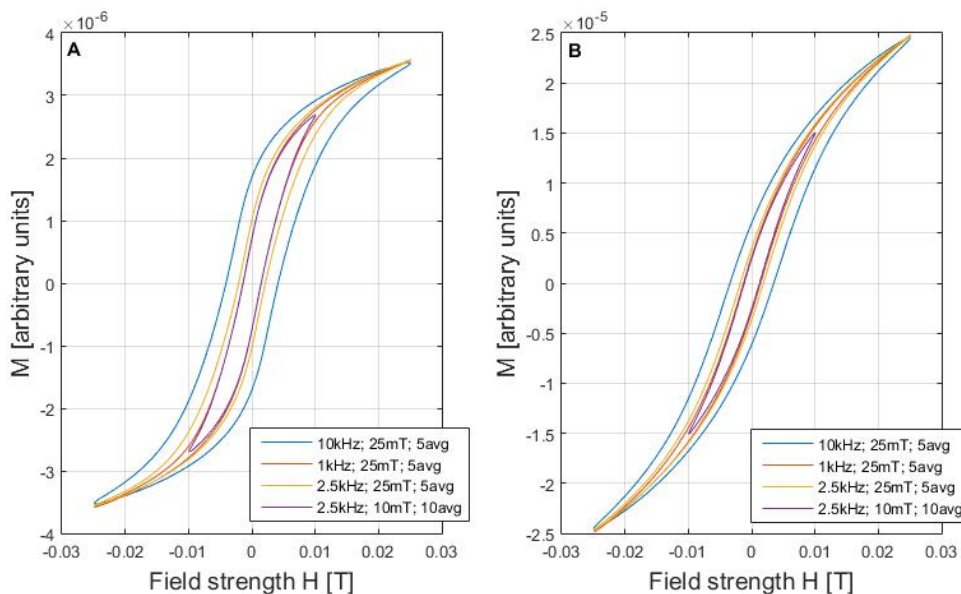


Figure 19: M curves of 10% Resovist (A) and freeze-dried Resovist (B). Measured by MPS for different measurement parameters.

All measured M curves consist of a closed hysteresis loop. Most importantly, the hysteresis loops close at the maximum measured field amplitude. For identical amplitudes, a higher frequency results in a wider hysteresis curve. The hysteresis width of the M curves generated at 1kHz and 25mT and at 2.5kHz and 10mT are identical. All of these observations can be made for both the liquid as the freeze-dried sample. The sole difference between the freeze-dried and liquid samples is, that the width of the hysteresis loop is wider for the liquid samples.

These observations can be explained by the behaviour of the magnetic moment in an alternating magnetic field. The magnetic moment of a superparamagnetic particle will attempt to align with the applied field. As the field changes, this moment will attempt to follow. As the field changes slower than the relaxation of the particle, the particle is able to keep up. Whenever the field changes faster than the relaxation time allows, the particle's moment will lag behind. The latter is what occurs in the magnetic particle spectrometer.

Whether a particle is capable of keeping up to the field, depends on the relaxation time, which is a physical property of the particle. It further depends on the rate of change of the magnetic field, dH/dt . For an ac magnetic field this thus depends on frequency, and also on the amplitude. Therefore, both an increased frequency, as well as an increased amplitude will result in an increase in lag.

The width of the hysteresis curve indicates the amount of lag occurring in a sample. A wider hysteresis curve is caused by more lag, which is caused by a too high frequency and/or amplitude. Since Brownian motion is limited in the dried sample, this sample is dominated by Néel relaxation, which is more rapid than Brownian relaxation. Therefore, the amount of hysteresis is less than that of the liquid sample.

Both SPaQ and the MPS use the same basic principle. Alternating the magnetic field induces a voltage equal to the derivative of the magnetization curve. As MPS uses relatively large amplitude dM/dH is determined for the fields from -25mT to 25mT in one period of the excitation field (assuming an amplitude of 25mT and ignoring the used averaging). SPaQ uses small amplitudes and therefore only finds dM/dH for the fields from -1.5mT to 1.5mT (assuming an amplitude of 1.5mT). Whenever a DC offset field is applied, the dM/dH curve around this offset field is measured. This is what happens in SPaQ.

As MPS uses high amplitudes and a high frequency, the magnetic moments easily lag behind the excitation field. SPaQ uses both a lower frequency and a lower amplitude, therefore lag is less likely to occur. Thus, sufficiently low frequencies of both systems should therefore result in identical dM/dH curves. A low enough frequency in MPS should result in a similar result as given by SPaQ, while an increased frequency in SPaQ should result in similar curves as those found in MPS.

As previously observed, the hysteresis width of the M curves generated at 1kHz and 25mT and at 2.5kHz and 10mT are identical. As the ratio of frequency to field amplitude is identical, this points to a direct relation between the width of the hysteresis curve and the ratio of frequency to field amplitude. However, as this was only observed for two measurements, this cannot be confirmed at this moment.

6 AC Susceptibility and Magnetorelaxometry for SPION analysis

While on the subject of SPION assessment and various methods for magnetic detection, two other systems will be briefly touched upon. These being the AC Susceptometer (ACS) and the Magnetic Relaxometer (MRX). Neither of these systems measures the dM/dH nor a magnetization curve. Therefore, these systems cannot directly be compared to SPaQ. However, due to the importance of the relaxation times of the SPIONs and the used frequency of the SPaQ and the MPS, MRX and ACS do have some relevance regarding the subject. This section will only discuss the relevance of both systems regarding the subject. Therefore, the physical background is merely touched upon.

In AC susceptibility the sample containing SPIONs is exposed to an alternating magnetic field of constant field strength amplitude. The frequency of the excitation signal is swept to find the complex magnetic susceptibility as a function of frequency. This curve can be fitted using a Debye model. By doing so, both the hydrodynamic size and the core size of the used superparamagnetic particle can be approximated. This is possible for both monodisperse, as well as polydisperse distributions [26].

In magnetic relaxometry (MRX) a 2mT signal is used to excite the SPIONs in the sample for 2 seconds. As this is switched off, all magnetic moments will revert to their natural, disordered state. By measuring this decay over time for 2 seconds, the effective relaxation time of the nanoparticles can be determined. For this, the measured relaxation curve does need to be fitted, as 2mT is not sufficient to reach saturation, extrapolation of the found curve is required. By subsequently fitting the found curve with the Moment Superposition Model (MSM), the hydrodynamic and core size of the sample can be found [27].

The dM/dH curve determined by the SPaQ can be used to determine the core size distribution of the used sample too [1]. As this is possible using MRX and ACS as well, this would allow these systems to be compared further. This value could also be determined using a transmission electron microscope (TEM). Thus comparing all systems and determining the validity of the used models.

7 Discussion

Several sections of this report already contained discussion regarding the physical occurrences measured by the SPaQ, VSM, and MPS. Also, all experimental results have previously been discussed. This section will therefore focus on the comparison of all systems regarding the purpose of SPaQ, as described in section 2.2.

The hypothesis that the temperature affected the measured dM/dH curves by SPaQ has been tested and partially confirmed. Temperature fluctuations throughout the system do affect the shape of the measured curves. However, this is not the sole cause. By introducing a waiting period of thirty minutes, the measured DiffMag does become reproducible. This is, up to an offset of 10mT. Errors beyond this field strength are most likely caused by filtering within the electronics of the system.

Using the constant shape at constant temperatures, a fit is used to estimate the proper height of the dM/dH curves. Treating SPaQ's output curves with this fit does return reproducible results. This fit has not been tested for validity and can only be considered a patch for an underlying problem. Potential solutions regarding this problem can be found in the recommendations, section 9.

One of SPaQ's purposes, is the quantification of SPIONs in an unknown sample for medical applications. Specifically, in lymph nodes. This purpose can be considered to be more practical, and will therefore be treated as such.

The SPaQ, VSM and MPS are all able to quantify the amount of SPIONs in a sample with reasonable accuracy. The effect of using a lymph node as medium containing the SPIONs has yet to be determined. The immobilization of SPIONs, only leaving Brownian relaxation, is a prerequisite for the VSM to be able to produce reliable results regarding quantification. The magnetization curve for liquid samples can be measured, but cannot be used to quantify the amount of particles within a sample. In the SPaQ and the MPS the immobilization of the particles merely has a dampening effect on the measured curves. As the degree of immobilization in a lymph node is not known, this would affect each system differently. As this uncertainty affects all systems, this is not an advantage of any either.

The larger sample holder of SPaQ does make it more suitable to fit a lymph node. The default MPS sample holder merely contains $150\mu L$, while the used sample sizes for the VSM were $15\mu L$. These impracticalities are easy to overcome by increasing the sample holder size of both systems. In fact, the VSM has previously been used to quantify the amount of SPIONs in lymph nodes [4].

Long measurement times are a drawback for the VSM in a medical setting. For low magnetic field magnitudes, too few data points are measured to be able to use the M curve's derivative for quantification. Therefore, the full magnetization curve needs to be plotted for quantification. Using an incremental measurement approach, the VSM can gather more data points in low fields. This would require an even longer measurement time though. The now used 30 minute measurement time could be reduced too, resulting in fewer data points. However the full curve cannot be constructed in the mere one second required for the SPaQ and MPS to quantify the amount of SPIONs in a sample.

SPaQ's close relation to the hand held probe using differential magnetometry should be kept in mind while comparing SPaQ to other systems. The connected purpose is to determine a DiffMag curve representative of the DiffMag values measured by the hand held probe. This would allow SPaQ to find suitable nanoparticles

for use in a clinical setting.

For this purpose, SPaQ has a clear advantage over the other two systems. VSM measurements result in a static magnetization curve. Also, at the magnetic field amplitudes used in the hand held probe, the VSM is only able to gather about ten measurement points. Therefore, the VSM is not suitable for the purpose of identifying suitable nanoparticles for DiffMag.

The SuperParamagnetic Quantifier should result in a curve suitable for this purpose, as settings are used which are optimized for the hand held probe. This is not the case for MPS. Even when using an identical frequency as in SPaQ, the relaxation of the particles is also affected by the used amplitude of the AC signal. Using a much smaller frequency in the MPS should result in an identical dM/dH curve.

Deviating from the comparison regarding the intended purpose of SPaQ, SPaQ and MPS can also be compared regarding their ability to detect core size distributions of SPION samples. For this purpose, it seems advantageous to use the MPS set-up as used at the Technical University of Braunschweig. Currently, the produced results using this system are more reliable, and the use of the frequency spectrum allows for analysis in an additional dimension. However, improvements of SPaQ as will be suggested in the recommendations could result in the reliability of SPaQ matching that of the MPS in the future.

For its intended purposes, it is advantageous to use the SuperParamagnetic Quantifier rather than Vibrating Sample magnetometry or Magnetic Particle Spectroscopy. However, both other systems currently outperform SPaQ in reliability and reproducibility.

8 Conclusion

Final purpose of this report is, to compare the SuperParamagnetic Quantifier to Vibrating Sample Magnetometry and Magnetic Particle Spectroscopy. Also, for this purpose, the cause of irreproducibility has been researched. Where the hypothesis was made that this cause was a temperature dependency.

It can be concluded that temperature does influence the resulting dM/dH curves. However, the temperature at which is measured is not as important. Instead, temperature fluctuations cause the shape of the dM/dH curve to be influenced. As to why this occurs, no conclusions can be drawn. Keeping the system at a constant temperature by the introduction of a waiting period of 30 minutes preceding each measurement removes the temperature dependency. The remaining drift is compensated by fitting the data with the derivative of the Langevin function. This method has yet to be validated.

SPaQ's output curves cannot be validated using either VSM or MPS as these methods rely on different physical principles. Vibrating Sample Magnetometry measures the static magnetization curve. Magnetic particle Spectroscopy measures the dynamic dM/dH curve. As SPaQ relies on the use of a low amplitude AC field, while the DC field is swept, this could be considered a mixture of both dynamic and static magnetization principles. SPaQ could result in identical curves as the MPS, however this would require the MPS to measure at much lower frequencies, which it is unable to at this moment.

For the purpose of using SPaQ to find suitable superparamagnetic iron oxide nanoparticles for the use in Differential Magnetometry, it is more suitable than either VSM or MPS. This because SPaQ is able to determine DiffMag values representative of those found by the hand held probe.

9 Recommendations

Both Differential Magnetometry and the SuperParamagnetic Quantifier can be considered young regarding research done on it. Therefore, possible recommendations are nearly unlimited. Therefore, this section is subdivided in a part regarding a continuation of the research described in this report, a part regarding the measurement sequence used in SPaQ, and a part on the hardware of the system.

9.1 Further comparison

As the effect of using different quantities of SPIONs in each system (SPaQ, VSM and ACS) seems clear, this has become less interesting. For the comparison of all systems, the behaviour of SPIONs in the respective excitation fields is most relevant. Specifically, behaviour considering the relaxation of magnetic moments. One could argue the measured magnetization curve and dM/dH curves should be identical whenever the relaxation of the particles is not able to lag behind the excitation signal. In the VSM, this can be achieved by using incremental changes of the magnetic field, rather than using a continuous approach. For MPS, the used frequency should be decreased to the point where the relaxation no longer lags behind the excitation field. As SPaQ uses smaller amplitudes than those used in MPS, this should already be the case.

Both the SPaQ and the MPS output their curves in arbitrary units. Converting these units to SI units would make comparison simpler. Obviously, removing the irreproducibility of SPaQ would too. Possibilities to do so are explored in the following subsections.

9.2 Measurement sequence

Figure 6 illustrates the excitation signal as currently used in SPaQ. As the m-file used to run this sequence is called *Langevinsweep*, this is also referred to as the sequence name. Based on the excitation sequence used in MPS at the University of Braunschweig, some improvements on this existing excitation signal can be suggested.

First of all, SPaQ only sweeps the DC signal from the negative maximum amplitude to the positive maximum amplitude. Effectively only measuring half the dM/dH curve. By sweeping the DC signal back again, the full curve could be constructed. Thus also ensuring the occurrence of hysteresis will be easier identified.

The excitation sequence can be further improved by measuring multiple periods of the DC sweep. Effectively, the curve would be measured more often. By averaging all output signals, the output curves should be more constant. This principle is also applied in MPS. Of course, the reference measurement must be averaged too. The resulting sequence would look like the one in figure 20A. In this example, only two averages are taken.

Of course, repeating the excitation signal would result in increased measurement times and thus increased heating. Therefore, the shortest possible measurement time should be determined. Preliminary experiments have shown that a measurement time as short as 0.1 second is sufficient for large Resovist samples ($150\mu L 100\% Resovist$). More extensive experiments are required to find a suitable measurement time for samples containing much smaller amount of Resovist.

Thereby allowing more repetitions of each measurement without heating the system too much. Also, the one second excitation signal at maximum amplitude should be reduced in time.

Another possibility is to use a stepwise increase of the DC offset field. This would be more accurate, as averaging multiple signals is only possible for an identical DC offset. The previously proposed sequence would not result in multiple dM/dH curves at an identical offset, as the DC offset was ever changing. Using a stepwise approach would resolve this. This is illustrated in figure 20B.

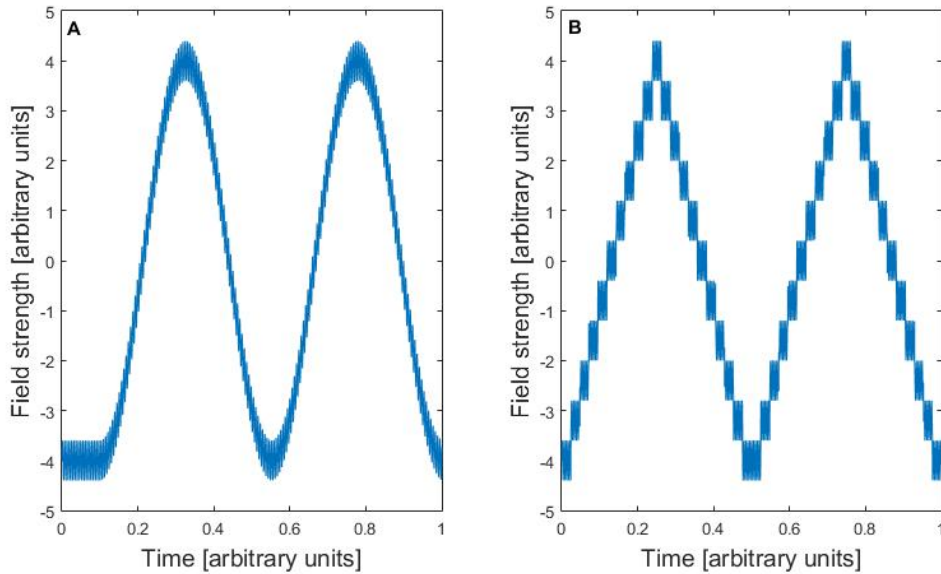


Figure 20: Proposed excitation sequences to replace Langevinsweep.m; a continuous repetition of each dM/dH measurement (A); a stepwise increase of the field offset (B).

9.3 SuperParamagnetic Quantifier

As SPaQ is but a first prototype, improvements can be made upon the software as well as the hardware. Although the hardware also includes the attached electrical circuits such as filters and amplifiers, these recommendations will focus on the set-up containing the coils. Specifically regarding the temperature distribution throughout the system.

The current (first) iteration uses passive cooling in the form of the oil bath. As mentioned before, the heat flow throughout the system is therefore limited by the heat capacity of the material containing the oil. Furthermore, heat flow from the excitation to the detection coil is barely inhibited. One could consider reverting to an active form of cooling. However, as this could lead to larger temperature fluctuations, another approach is recommended.

A second iteration of the SuperParamagnetic Quantifier, based on the magnetic particle spectrometer at the Technical University of Braunschweig could be manufactured. This design, as can be seen in figure 21, is more open than the SPaQ.

Most importantly, insulation around each coil is required. A suitable material needs to be selected to ensure no heat is transferred from the excitation coil to the

induction coil. As discussed before, heating of the coils should not affect the excitation field, or the induced voltage. This approach prevents temperature fluctuations, while the currently used oil bath ensures the opposite. Additionally, the induction coils should be wrapped around a well conducting (ceramic) material to divert heat leakage to the sample.

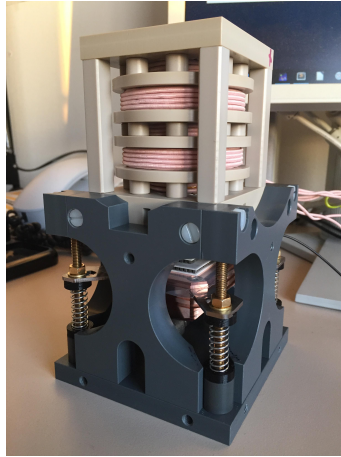


Figure 21: The magnetic particle spectrometer at the Technical University of Braunschweig [21].

Of course the recommended set-up cannot be identical to that of the MPS, as the sample holder of SPaQ is required to be much larger to be able to hold a lymph node. The MPS system is able to heat or cool it's sample using a Peltier element. As a larger sample holder is used in SPaQ, this is not a requirement, as the sample is unlikely to be affected by the system's temperature.

10 Acknowledgements

I would like to acknowledge Melissa van de Loosdrecht (MSc) for her guidance and supervision. Furthermore, I would like to acknowledge the Institut für Elektrische Messtechnik und Grundlagen der Elektrotechnik for their knowledge and the opportunity to utilize their Magnetic Particle Spectrometer, AC Susceptometer and Magnetorelaxometer.

References

- [1] Waanders S, Visscher M, Wildeboer RR, Oderkerk TOB, Krooshoop HJG, ten Haken B. A handheld SPIO-based sentinel lymph node mapping device using differential magnetometry. *Physics in Medicine and Biology*. 2016;61(22):8120–8134.
- [2] Thill M, Kurylcio A, Welter R, van Haasteren V, Grosse B, Berclaz G, et al. The Central-European SentiMag study: Sentinel lymph node biopsy with superparamagnetic iron oxide (SPIO) vs. radioisotope. *The Breast*. 2014;23(2):175–179.
- [3] Visscher M, Waanders S, Krooshoop HJG, ten Haken B. Selective detection of magnetic nanoparticles in biomedical applications using differential magnetometry. *Journal of Magnetism and Magnetic Materials*. 2014;365:31–39.
- [4] Visscher M, Pouw JJ, van Baarlen J, Klaase JM, ten Haken B. Quantitative Analysis of Superparamagnetic Contrast Agent in Sentinel Lymph Nodes Using Ex Vivo Vibrating Sample Magnetometry. *IEEE Transactions on Biomedical Engineering*. 2013;60(9):2594–2602.
- [5] Panagiotopoulos N, Vogt F, Barkhausen J, Buzug TM, Duschka RL, Lüdtke-Buzug K, et al. Magnetic particle imaging: current developments and future directions. *International Journal of Nanomedicine*. 2015;p. 3097.
- [6] Biederer S, Knopp T, Sattel TF, Lüdtke-Buzug K, Gleich B, Weizenecker J, et al. Magnetization response spectroscopy of superparamagnetic nanoparticles for magnetic particle imaging. *Journal of Physics D: Applied Physics*. 2009;42(20):205007.
- [7] Giuliano AE, Gangi A. Sentinel Node Biopsy and Improved Patient Care. *The Breast Journal*. 2014;21(1):27–31.
- [8] Anninga B, Ahmed M, Van Hemelrijck M, Pouw J, Westbroek D, Pinder S, et al. Magnetic sentinel lymph node biopsy and localization properties of a magnetic tracer in an in vivo porcine model. *Breast Cancer Research and Treatment*. 2013;141(1):33–42.
- [9] Ahmed M, Purushotham AD, Douek M. Novel techniques for sentinel lymph node biopsy in breast cancer: a systematic review. *The Lancet Oncology*. 2014;15(8):e351–e362.

- [10] Krag DN, Anderson SJ, Julian TB, Brown AM, Harlow SP, Costantino JP, et al. Sentinel-lymph-node resection compared with conventional axillary-lymph-node dissection in clinically node-negative patients with breast cancer: overall survival findings from the NSABP B-32 randomised phase 3 trial. *The Lancet Oncology*. 2010;11(10):927–933.
- [11] Magnetic Detection & Imaging. Differential magnetometry to detect sentinel lymph nodes in laparoscopic procedures; 2017. Available from: <https://www.utwente.nl/en/tnw/mdi/research/Magnetic%20Detection/laparoscopy-project/>.
- [12] Van de Loosdrecht M, Waanders S, Wildeboer R, Krooshoop E, Ten Haken B. Differential magnetometry to detect sentinel lymph nodes in laparoscopic procedures (poster); 2017.
- [13] Deatsch AE, Evans BA. Heating efficiency in magnetic nanoparticle hyperthermia. *Journal of Magnetism and Magnetic Materials*. 2014;354:163–172.
- [14] Giancoli DC. *Physics for scientists and engineers*. 4th ed. Pearson;.
- [15] Tipler PA, Mosca G. *Physics for scientists and engineers*. 6th ed. W.H. Freeman; 2008.
- [16] Baronzio GF, Hager ED. *Hyperthermia in Cancer Treatment: A Primer*. 1st ed.;.
- [17] C F Chan D, B Kirpotin D, A Bunn P. Synthesis and evaluation of colloidal magnetic iron oxides for the site-specific radiofrequency-induced hyperthermia of cancer. *Journal of Magnetism and Magnetic Materials*. 1993;122(1-3):374–378.
- [18] Javidi M, Heydari M, Attar MM, Haghpanahi M, Karimi A, Navidbakhsh M, et al. Cylindrical agar gel with fluid flow subjected to an alternating magnetic field during hyperthermia. *International Journal of Hyperthermia*. 2014;31(1):33–39.
- [19] Jordan A, Wust P, Fählin H, John W, Hinz A, Felix R. Inductive heating of ferromagnetic particles and magnetic fluids: Physical evaluation of their potential for hyperthermia. *International Journal of Hyperthermia*. 1993;9(1):51–68.
- [20] Mahmoudi M, Sahraian MA, Shokrgozar MA, Laurent S. Superparamagnetic Iron Oxide Nanoparticles: Promises for Diagnosis and Treatment of Cancer. *ACS Chemical Neuroscience*. 2011;2(3):118–140.
- [21] Draack S, Viereck T, Kuhlmann C, Schilling M, Ludwig F. Temperature-dependent MPS measurements. *International Journal on Magnetic Particle Imaging*. 2017;3.
- [22] Lubell MS, Venturino AS. Vibrating Sample Magnetometer. *Review of Scientific Instruments*. 1960;31(2):207–208.
- [23] Dodrill BC. *Low Moment Measurement with a Vibrating Sample Magnetometer*. Lake Shore Cryotronics, Inc;.

- [24] Jin R, Moreira Teixeira LS, Dijkstra PJ, van Blitterswijk CA, Karperien M, Feijen J. Chondrogenesis in injectable enzymatically crosslinked heparin/dextran hydrogels. *Journal of Controlled Release*. 2011;152(1):186–195.
- [25] Ludwig F, Wawrzik T, Yoshida T, Gehrke N, Briel A, Eberbeck D, et al. Optimization of Magnetic Nanoparticles for Magnetic Particle Imaging. *IEEE Transactions on Magnetics*. 2012;48(11):3780–3783.
- [26] Ludwig F, Guillaume A, Schilling M, Frickel N, Schmidt AM. Determination of core and hydrodynamic size distributions of CoFe₂O₄ nanoparticle suspensions using ac susceptibility measurements. *Journal of Applied Physics*. 2010;108(3):033918.
- [27] Ludwig F, Remmer H, Kuhlmann C, Wawrzik T, Arami H, Ferguson RM, et al. Self-consistent magnetic properties of magnetite tracers optimized for magnetic particle imaging measured by ac susceptometry, magnetorelaxometry and magnetic particle spectroscopy. *Journal of Magnetism and Magnetic Materials*. 2014;360:169–173.

List of Figures

1	Principle of a sentinel lymph node biopsy. A dye and tracer are injected at the tumor location and travel through the lymphatic system towards the sentinel lymph nodes, indicated in blue [1].	4
2	Set-up of the SuperParamagnetic Quantifier at the University of Twente.	6
3	Magnetization due to an applied field for a superparamagnetic nanoparticle and a diamagnetic material [1].	7
4	Néel relaxation (A) and Brown relaxation (B) over time [13].	7
5	Concept of differential magnetometry [3].	9
6	The sequence as used in SPaQ to determine the dM/dH curve.	10
7	The measured dM/dH curve (left) and the integrated M of H curve (right).	10
8	Measured output curves for identical measurements at different starting temperatures. In these measurements, the temperature was not kept constant throughout the measurement and system.	15
9	Measured output curves for identical measurements at 25°C (A); 28°C (B); 31°C (C) and the DiffMag values of these measurements (D).	16
10	The maxima of all measurements for the constant temperatures at which they are measured. Also shown is a linear fit of the plotted data.	17
11	Procedure for fit compensation of the measured dM/dH curves by SPaQ; the measured data (A); deletion of all data beyond ±10mT and the addition of data points at −1000mT and 1000mT (B); fit with the derivative of the Langevin function for different heights of the original data, while the added data points remain unaltered (C); data compensated for fit (D).	18

12	Corrected data for the Langevin fit; the unaltered data for three measurements at different constant temperatures (A); the same data compensated for the fit (B). As the data beyond 10mT is not used for the fitting, it is not displayed in the compensated plot.	19
13	dM/dH curves as measured by SPaQ for liquid and gelated Resovist samples (A) and the DiffMag values associated with this curve (B).	23
14	M curve results of the vibrating sample magnetometer; M curves Resovist samples in a Dextran hydrogel (A); M curves liquid Resovist samples (B); M curves of reference samples (C); Three selected M curves for low field amplitudes (D).	24
15	Side by side comparison of M curves generated by integrating SPaQ measurement results (A) and M curves determined by vibrating sample magnetometry.	25
16	Principle of Magnetic Particle Spectroscopy; the excitation signal drives an alternating magnetic field (a); the magnetic moment of SPIONs follow this field according to the magnetization curve (b); the sinusoidal excitation signal results in a changed magnetic moment over time (c); the derivative of this magnetization is measured as a voltage (d); taking the Fourier transform of this signal results in the harmonic signal spectrum (e) [6].	27
17	dM/dH curves as determined by the SPaQ for multiple concentrations of Resovist and freeze-dried Resovist.	29
18	dM/dH curves measured by MPS for different frequencies, amplitudes and number of averages; 10kHz, 25mT, 5avg (A); 1kHz, 25mT, 5avg (B); 2.5kHz, 25mT, 5avg (C); 2.5kHz, 10mT, 10avg (D).	29
19	M curves of 10% Resovist (A) and freeze-dried Resovist (B). Measured by MPS for different measurement parameters.	30
20	Proposed excitation sequences to replace Langevinsweep.m; a continuous repetition of each dM/dH measurement (A); a stepwise increase of the field offset (B).	37
21	The magnetic particle spectrometer at the Technical University of Braunschweig [21].	38

List of Tables

1	DiffMag values at an offset of 5mT as measured by SPaQ and saturation magnetization as measured by the VSM.	23
2	Temperature measurements for measurements conducted at different starting temperatures consecutively executed.	43
3	Temperature measurements for measurement 1 to 13. Each measurement was preceded by a waiting period of a couple of hours for the system to reach thermal equilibrium.	43

A Temperature measurements

Section 3 explored the influence of the temperature on the results produced by the SPaQ. For this purpose, temperature measurements were recorded both before and after the experiments without temperature control and at constant temperature. These are displayed in table 2 and 3 respectively.

Table 2: Temperature measurements for measurements conducted at different starting temperatures consecutively executed.

$T_{set}[^{\circ}C]$	$T_{mat}[^{\circ}C]$	$T_{heater}[^{\circ}C]$	$T_{mat,end}[^{\circ}C]$	$T_{heater,end}[^{\circ}C]$
25 ± 0.2	25.2	25.0	25.5	25.0
25 ± 0.2	25.4	25.0	25.6	24.9
25 ± 0.2	25.6	25.0	25.9	25.0
25 ± 0.2	25.8	25.0	26.0	25.0
25 ± 0.2	26.0	25.0	26.1	25.0
30 ± 0.2	30.0	29.9	30.2	29.9
30 ± 0.2	30.1	29.9	30.2	29.9
30 ± 0.2	30.2	29.9	30.3	29.9
30 ± 0.2	30.3	29.8	30.5	30.1
30 ± 0.2	30.4	30.4	30.7	30.1
38 ± 0.2	38.2	37.8	38.3	37.8
38 ± 0.2	38.4	37.9	38.6	38.0
38 ± 0.2	38.5	38.0	38.7	38.0
38 ± 0.2	38.9	38.0	38.9	38.0
38 ± 0.2	39.0	38.0	39.2	37.9
45 ± 0.2	45.7	44.6	45.8	44.8
45 ± 0.2	45.9	45.0	46.0	44.7
45 ± 0.2	45.8	45.1	46.1	44.6
45 ± 0.2	46.0	44.8	46.1	44.7

Table 3: Temperature measurements for measurement 1 to 13. Each measurement was preceded by a waiting period of a couple of hours for the system to reach thermal equilibrium.

	$T_{set}[^{\circ}C]$	$T_{mat}[^{\circ}C]$	$T_{heater}[^{\circ}C]$	$T_{sample}[^{\circ}C]$	$T_{mat,end}[^{\circ}C]$	$T_{heater,end}[^{\circ}C]$
1	38 ± 0.2	31.0	31.2	30.16	31.1	31.2
2	38 ± 0.2	30.9	31.3	30.05	31.1	31.3
3	38 ± 0.2	31.6	31.9	30.80	31.5	32.0
4	45 ± 0.2	31.2	31.8	30.49	31.4	31.8
5	25 ± 0.2	24.5	25.0	24.62	24.9	25.0
6	25 ± 0.2	24.4	25.2	23.90	24.3	25.0
7	25 ± 0.2	24.3	25.0	23.71	24.3	25.0
8	25 ± 0.2	24.2	24.9	23.77	24.3	25.0
9	25 ± 0.2	24.3	25.0	23.54	24.3	25.0
10	28 ± 0.2	27.0	27.8	26.41	27.4	27.8
11	28 ± 0.2	27.1	28.0	26.41	27.2	28.0
12	28 ± 0.2	27.0	28.0	26.39	27.2	27.9
13	28 ± 0.2	27.1	28.0	26.42	27.0	27.9